Fgd5 identifies hematopoietic stem cells in the murine bone marrow

Fgd5 identifies hematopoietic stem cells in the murine bone marrow

Roi Gazit,[1,2] Pankaj K. Mandal,[1,2] Wataru Ebina,[1,2] Ayal Ben-Zvi,[5] César Nombela-Arrieta,[3] Leslie E. Silberstein,[2,3,6] Derrick J. Rossi[1,2,4,6]

[1]Department of Stem Cell and Regenerative Biology, Harvard University, Cambridge, MA 02138
[2]Program in Cellular and Molecular Medicine, Division of Hematology/Oncology and [3]Division of Transfusion Medicine, Department of Laboratory Medicine, Boston Children's Hospital, MA 02116
[4]Department of Pediatrics, [5]Department of Neurobiology, Harvard Medical School, Boston MA 02115
[6]Harvard Stem Cell Institute, Cambridge, MA 02138

Hematopoietic stem cells (HSCs) are the best-characterized tissue-specific stem cells, yet experimental study of HSCs remains challenging, as they are exceedingly rare and methods to purify them are cumbersome. Moreover, genetic tools for specifically investigating HSC biology are lacking. To address this we sought to identify genes uniquely expressed in HSCs within the hematopoietic system and to develop a reporter strain that specifically labels them. Using microarray profiling we identified several genes with HSC-restricted expression. Generation of mice with targeted reporter knock-in/knock-out alleles of one such gene, *Fgd5*, revealed that though *Fgd5* was required for embryonic development, it was not required for definitive hematopoiesis or HSC function. *Fgd5* reporter expression near exclusively labeled cells that expressed markers consistent with HSCs. Bone marrow cells isolated based solely on *Fgd5* reporter signal showed potent HSC activity that was comparable to stringently purified HSCs. The labeled fraction of the *Fgd5* reporter mice contained all HSC activity, and HSC-specific labeling was retained after transplantation. Derivation of next generation mice bearing an *Fgd5-CreERT2* allele allowed tamoxifen-inducible deletion of a conditional allele specifically in HSCs. In summary, reporter expression from the *Fgd5* locus permits identification and purification of HSCs based on single-color fluorescence.

CORRESPONDENCE
Derrick J. Rossi:
derrick.rossi@childrens.harvard.edu

Abbreviations used: GEF, guanine nucleotide exchange factor; HSC, hematopoietic stem cell; MPP, multipotent progenitor; LSK, Lineage$^-$Sca1$^+$c-Kit$^+$; QC, quality control.

Hematopoietic stem cells (HSCs) function to maintain blood homeostasis throughout life via their unique ability to differentiate into all blood cell types and to self-renew. These properties, along with the robust ability of HSCs to engraft myeloablated recipients in the setting of BM transplantation, have established the clinical paradigm for therapeutic stem cell use (Weissman, 2000).

Originally described by Till and McCulloch (1961), HSCs were first experimentally defined by their ability to form macroscopic colonies in the spleens (CFU-S) of irradiated recipients after BM transplantation that histological examination revealed contained multiple blood lineages, and cytological examination revealed were clonally derived (Becker et al., 1963). Together with the demonstration that a subset of CFU-S colonies had the potential to reform colonies when transplanted into secondary recipients (Siminovitch et al., 1963), the defining properties of hematopoietic stem cells—multipotency and self-renewal—were established. In the 50 yr since these seminal studies were conducted, the experimental study of HSCs has flourished, leading to a profound level of understanding of their biology. These efforts were enabled through the development of several in vivo and in vitro assays that permitted evaluation of HSC self-renewal and multilineage potential, and by methods that allowed purification of HSCs by FACS. HSCs were initially reported to be enriched within the Thy1^{low}Lineage$^-$ fraction of the murine BM (Muller-Sieburg et al., 1986), and subsequently cells with a Thy1^{low}Lineage$^-$Sca1$^+$

R. Gazit and P.K. Mandal contributed equally to this paper.
R. Gazit's present address is the Shraga Segal Dept. of Microbiology, Immunology, and Genetics, BGU Center for Regenerative Medicine & Stem Cells, National Institute for Biotechnology in the Negev, Ben-Gurion University in the Negev, Be'er-Sheva, Israel.

The Rockefeller University Press $30.00
J. Exp. Med. 2014 Vol. 211 No. 7 1315-1331
www.jem.org/cgi/doi/10.1084/jem.20130428

The Journal of Experimental Medicine

immunophenotype were shown to possess long-term multilineage repopulating activity (Spangrude et al., 1988). The immunophenotype of HSCs was further refined, culminating with the demonstration that single cells purified from the Lineage$^-$Sca1$^+$c-kit$^+$ (LSK)CD34$^{-/low}$ fraction of the BM of adult mice could function to long-term multilineage reconstitute irradiated recipients at the clonal level (Osawa et al., 1996). Additional cell surface markers that have also been used to enrich for HSC activity include: CD105 (Chen et al., 2002), Flk2/Flt3 (Christensen and Weissman, 2001), CD201/PROCR (Balazs et al., 2006), ESAM (Ooi et al., 2009; Yokota et al., 2009), and CD150, CD48, and CD244 (Kiel et al., 2005a) among others. In addition to immunophenotype, intravital dye efflux activity has also proven to be an effective strategy for enriching for HSC activity (Bertoncello et al., 1985; Wolf et al., 1993; Goodell et al., 1996).

Although immunophenotype combined with flow cytometry has become the principle technique used for identifying and studying diverse cells types, genetically engineered reporter strains have also enabled the identification and study of other cell types, including tissue-specific stem cells from other organs. For example, rapidly cycling intestinal stem cells were identified with the use of an *Lgr5* reporter (Barker et al., 2007), whereas a population of more slowly cycling stem cells in the intestinal crypt were marked with a reporter for telomerase (Montgomery et al., 2011). In the developing embryo, reporter strains for Isl1 (Laugwitz et al., 2005) and WT1 (Zhou et al., 2008) have been combined with lineage-tracing experiments to identify cardiac progenitors in the developing heart. In the skin, a Tet-inducible H2B-GFP reporter stain was used in conjunction with a keratinocyte-specific driver to isolate label-retaining stem cells in the epidermis (Tumbar et al., 2004). A similar H2B-GFP label retention strategy was later used by two independent groups to explore the turnover of HSCs, showing that a label-retaining population of cells with potent HSCs activity resides in a state of prolonged dormancy during steady-state homeostasis (Wilson et al., 2008; Foudi et al., 2009). Importantly, depending on vector design, introducing reporter cassettes into specific genomic loci (knock-in) can also lead to the disruption of the targeted gene, permitting analysis of the null (knockout) genotype when targeted alleles are crossed to homozygosity.

With the goals of identifying novel genes that could be used to specifically report on HSC activity within the murine BM, we performed a system-wide microarray screen of hematopoietic stem, progenitor, and effector cells, and identified a set of genes whose expression was highly restricted to the HSC compartment. Generation of mice with targeted reporter knock-in/knock-out alleles at three of the identified genes, *Sult1a1*, *Clec1a*, and *Fgd5* revealed that whereas knockout of *Sult1a1* and *Clec1a* were viable and had normal HSC function, nullizygosity of *Fgd5* was embryonic lethal at midgestation, though the generation and function of definitive HSCs was not affected by loss of *Fgd5*. Of the three reporter alleles, only *Fgd5* explicitly marked immunophenotypic HSCs in the adult marrow at steady state and after transplantation. BM cells isolated based solely on reporter signal of the *Fgd5* reporter mice showed robust HSC activity, with all stem cell activity residing within the labeled fraction. These results demonstrate that HSCs can be identified and purified from the BM of *Fgd5* reporter mice by single color fluorescence. Finally, the development of *Fgd5-CreERT2* mice permitting inducible deletion of Floxed alleles specifically in HSCs represents an invaluable genetic resource for exploring gene function in HSC biology.

RESULTS

Systems-wide microarray screen identifies genes with HSC-restricted expression in the adult hematopoietic system

To identify genes specifically expressed in HSCs within the hematopoietic system, we compiled the expression profiles of 37 different hematopoietic cell types comprising the vast majority of hematopoietic progenitor and effector cells (Fig. 1 A). These datasets include published microarray data from our group and others that were carefully curated from publicly available databases. As many of these datasets were generated in different laboratories, we subjected them to a number of quality control (QC) measures in accordance with current standards using the ArrayQualityMetrics package of R/Bioconductor. In total, 122 expression profiles passed QC and were normalized together in a single database. Using this database, we were readily able to identify genes that showed highly restricted expression in diverse hematopoietic cell types (Fig. 1 B). Analysis of such cell type–specific gene lists indicated that previously established and validated cell type–specific genes could be identified (Fig. 1 B). These included genes known to mediate critical functions in specific cell types, as well as genes whose products are routinely used to phenotypically define different cell types with no known function in the specific cell type (Fig. 1 B). For example, *Ncr1*, which is critical in NK cells (Gazit et al., 2006), *Bcl11b*, which is involved in specifying T cell identity (Wakabayashi et al., 2003), and the adult α-globin in erythroblasts (Pászty et al., 1995) were highly restricted to these cells in our database (Fig. 1 B). Similar results were obtained for other hematopoietic cell types and, in all cases the cell type–specific genes were associated with a very high degree of statistical confidence due to the fact that only FACS-purified cells were used in the generation of the data, and also due to the large number of samples and biological replicates analyzed (Tables S1 and S2).

We next sought to identify genes predominantly expressed in HSCs (immunopurified as LSKFlk2$^-$CD34$^{low/-}$) in comparison to their downstream progenitor and effector progeny. This analysis identified 323 probe sets corresponding to 235 unique annotated genes with highly restricted expression in HSCs (Fig. 1 C, Fig. S1, and Table S2). This list overlapped significantly with the results of previous studies in which expression profiling of different hematopoietic cell types has been used to define HSC transcriptional signatures and explore their biology (Chambers et al., 2007a; Gazit et al., 2013; Fig. 1 D). Interestingly, many of the genes we identified were

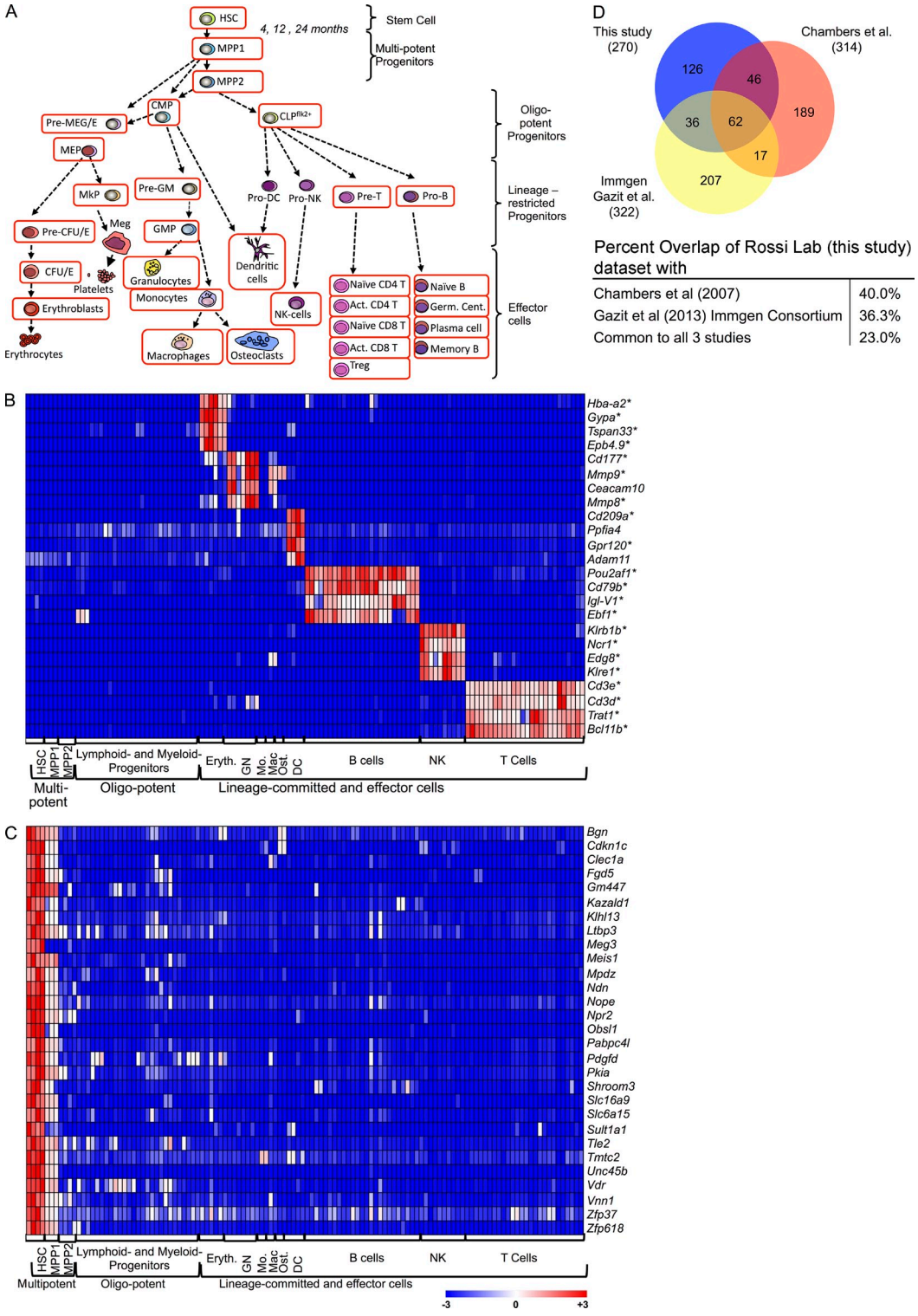

Figure 1. Identification of HSC-specific genes. (A) Schematic representation of the hematopoietic hierarchy showing cell types with expression profiles used in this study framed in red. (B) Heat map showing relative expression (from red, high, to blue, low) of genes identified as cell type specific in the indicated cell types, with asterisks (*) marking genes with well-established roles in the given cell type. (C) Heat map showing relative expression of representative genes identified as HSC-specific (for complete list see Fig. S1). (D) Venn diagram of HSC-enriched gene sets published in Gazit et al. (2013) (2013), Chambers et al. (2007a), and this study. Genes expressed >2.3-fold higher in HSCs relative to downstream populations examined in each study were selected from the current study and also the Chambers et al. (2007a) dataset. Percentage overlap of our HSC-enriched gene set with others is presented on the bottom.

also expressed at low levels in multipotent progenitors (MPP1s), which represent the most proximal progenitor to HSCs and have previously been referred to in the literature as short-term HSCs (ST-HSCs; Fig. 1 C). Among the HSC-enriched genes were several that encode proteins with well-established functional roles in HSC biology, such as *Cdkn1c* (Matsumoto et al., 2011; Zou et al., 2011), *Meis1* (Pineault et al., 2002), and *Ndn* (Kubota et al., 2009), in addition to many genes that have not yet been reported to have a functional role in HSC biology. We chose to focus on three genes of this latter group, *Clec1a*, *Fgd5*, and *Sult1a1*, which showed highly restricted expression in our database (Fig. 1 C). In addition to expression specificity, these genes were selected, in part, based on consideration of their genomic structure (intron/exon, repetitive elements), which suggested that they would be amenable to targeting by homologous recombination. Of these, *Clec1a* encodes a C-type lectin type II transmembrane receptor that has been shown to be expressed in human and rat dendritic and endothelial cells (Colonna et al., 2000; Sobanov et al., 2001; Thebault et al., 2009), and has been reported to play an immunomodulatory role in allograft tolerance in rats (Thebault et al., 2009). *Sult1a1* encodes a cytosolic transferase studied in human cells for its ability to conjugate sulfate to various phenolic substrates (Wilborn et al., 1993; Raftogianis et al., 1997; Hildebrandt et al., 2009). *Fgd5* encodes a protein predicted to have GTP-exchange (guanine nucleotide exchange factor [GEF]) activity that has been studied exclusively in the context of endothelial cell biology (Cheng et al., 2012; Kurogane et al., 2012). To our knowledge, *Fgd5*, *Clec1a,* and *Sult1a1* have not previously been studied in the context of HSC biology. Collectively, these results demonstrate that expression of *Fgd5*, *Clec1a,* and *Sult1a1* is predominantly confined to HSCs in the adult hematopoietic system.

Immunophenotypic HSCs are labeled by mCherry in *Fgd5*$^{mCherry/+}$ mice

To generate reporter mice and begin to explore the possible roles for *Clec1a*, *Sult1a1*, and *Fgd5* in HSC biology, constructs were made to target each locus by homologous recombination in embryonic stem (ES) cells using a knock-in/knock-out strategy. In all cases, constructs were designed to place a fluorescence reporter cassette (either mCherry into *Fgd5*, or eGFP•CreERT2 into *Clec1a* and *Sult1a1*) in-frame with the protein coding sequence that would be expected to be expressed under endogenous regulatory control. At the same time, correct targeting of the loci is expected to generate null alleles for each of the genes. Sequence verified targeting constructs were introduced into ES cells derived from C57BL/6 mice, correctly targeted ES cell clones were identified by Southern blotting, and germline transmission of the targeted alleles was established (not depicted).

To characterize the utility of the targeted alleles to label HSCs, we isolated BM cells from young adult *Fgd5*$^{mCherry/+}$, *Sult1a1*$^{GFP/+}$ and *Clec1a*$^{GFP/+}$ mice and control littermates and immunostained for HSCs using a panel of well-defined markers (LSKCD48$^-$CD150$^+$). Disappointingly, the BM of young adult *Clec1a*$^{GFP/+}$ mice showed almost negligible expression in HSCs, whereas HSCs identified from the BM of *Sult1a1*$^{GFP/+}$ mice were completely negative for reporter fluorescence (Fig. 2 A). In contrast, immunophenotypic HSCs from the *Fgd5*$^{mCherry/+}$ mice were almost uniformly positive for reporter signal (mCherry; Fig. 2 A). Although there could be several explanations for the absence of signal in HSCs of *Clec1a*$^{GFP/+}$ and *Sult1a1*$^{GFP/+}$ mice, we focused on the *Fgd5*$^{mCherry/+}$ mice for further characterization.

Whereas *Fgd5*$^{mCherry/+}$ mice clearly showed labeling of immunophenotypic HSCs, we sought to further determine the spectrum of BM cells expressing mCherry. To address this, we gated BM cells from the *Fgd5*$^{mCherry/+}$ mice into mCherry$^+$ and mCherry$^-$ fractions, and then determined the immunophenotype of these cells by co-staining with a panel of markers. This analysis revealed that in contrast to mCherry$^-$ cells, a significant fraction of the mCherry$^+$ cells were negative for the lineage markers associated with mature blood cells (B220, Mac1, GR-1, Ter119, CD3, CD4, and CD8); positive for c-Kit and Sca1; negative for CD48; and positive for CD150 (Fig. 2 B). By gating sequentially through these markers, the vast majority of the mCherry$^+$ cells of *Fgd5*$^{mCherry/+}$ BM co-stained with markers of immunophenotypic HSCs (LSKCD48$^-$CD150$^+$; Fig. 2 B, bottom).

Our expression profiling data showed that whereas *Fgd5* expression in the murine BM was almost exclusively restricted to HSCs, low-level expression was also detected in multipotent progenitor cells. To examine this, we stained the BM of *Fgd5*$^{mCherry/+}$ mice with several different marker combinations that are commonly used to identify HSCs and discriminate them from multipotent progenitor cell subsets within the primitive LSK fraction of the murine BM. Using markers associated with the "Slam code" (Kiel et al., 2005b), the vast majority of HSCs (LSKCD150$^+$CD48$^-$) were fluorescently labeled (Fig. 2 C). In contrast, the most proximal multipotent progenitors (LSKCD150$^-$CD48$^-$) showed low-level expression of the reporter, whereas the more distal LSKCD150$^-$CD48$^+$ progenitors were predominantly negative. Similarly, when CD34 and Flk2 were used to immunophenotypically define HSCs and multipotent progenitors (Osawa et al., 1996; Christensen and Weissman, 2001; Rossi et al., 2005), HSCs (LSKFlk2$^-$CD34$^-$) were largely positive, whereas the MPP1/ST-HSC (LSKFlk2$^-$CD34$^+$) population expressed lower levels of signal, and the MPP2 subset (LSKFlk2$^+$CD34$^+$) showed very little signal (Fig. 2 D), consistent with our microarray data (Fig. 1). Similar results were found using other marker immunophenotypic strategies to identify HSCs and multipotent progenitors including PROCR/CD201 (Balazs et al., 2006; Fig. 2 E) and ESAM (Ooi et al., 2009; Yokota et al., 2009; Fig. 2 F). Collectively, these results indicate that immunophenotypic HSCs are almost exclusively labeled in the BM of *Fgd5*$^{mCherry/+}$ mice.

Fgd5 deficiency does not impair HSC function and is not required for definitive hematopoiesis

Because the targeting of the *Fgd5* locus places a mCherry cassette into the first exon of the *Fgd5* coding region and is

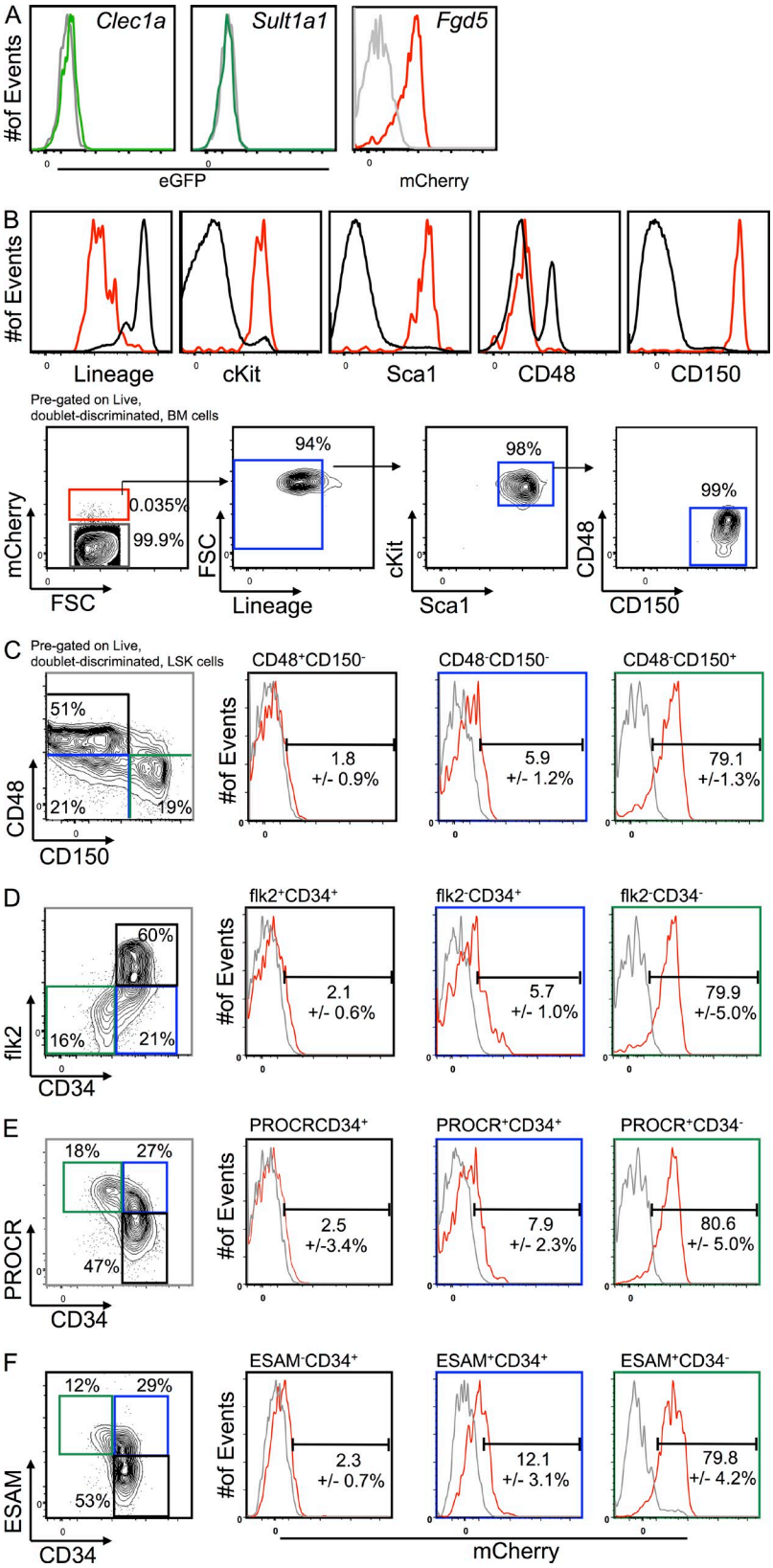

Figure 2. Reporter-labeled cells in BM of *Fgd5*$^{mCherry/+}$ mice are synonymous with immunophenotypic HSCs. (A) Histograms (colored) of reporter expression within immunophenotypic HSCs (LSKCD48$^-$CD150$^+$) from the BM of mice targeted at *Clec1a*^{eGFP}, *Sult1a1*^{eGFP}, and *Fgd5*^{mCherry} in comparison to the wild-type background (gray). (B) BM mCherry$^+$ (red histograms) and mCherry$^-$ (black histograms) cells of *Fgd5*$^{mCherry/+}$ mice co-stained and gated individually (top) or sequentially (bottom) through lineage (Ter119, Mac-1, Gr-1, B220, CD3, CD4, and CD8), c-Kit, Sca1, CD48, and CD150. (C–F) Sub-fractionation of primitive LSK cells from *Fgd5*$^{mCherry/+}$ (red histograms) or *Fgd5*$^{+/+}$ (gray histograms) mice into immunophenotypic HSCs (right, green gates) and multipotent progenitors (blue and black gates) by (C) CD150 and CD48, (D) CD34 and flk2, (E) PROCR and CD34, and (F) ESAM and CD34. Percentage mCherry$^+$ ± SD is shown and a minimum of $n = 3$ mice for each stain were analyzed.

predicted to generate a null allele, we wanted to determine if inactivation of one or both *Fgd5* alleles would affect HSC function. To address this in the setting of *Fgd5* heterozygosity, we competitively transplanted 10^6 BM cells from *Fgd5*$^{mCherry/+}$ or wild-type (*Fgd5*$^{+/+}$) control littermates (CD45.2) against 1×10^6 wild-type BM cells (CD45.1) into lethally irradiated

congenic recipients (CD45.1). Transplant recipients were bled at monthly intervals and reconstitution of CD45.2 test cells and their contribution to myeloid lineage granulocytes, macrophages/monocytes, lymphoid lineage B cells, and T cells, was determined (Fig. 3 A). This showed that *Fgd5* heterozygosity had no adverse effect on HSC function in respect to total repopulation or lineage potential in primary (1°) transplant recipients. To further challenge the *Fgd5*$^{mCherry/+}$ and wild-type HSCs, serial transplantation into secondary (2°) recipients was performed. Peripheral blood analysis up to 20 wk after transplant revealed that HSCs derived from both *Fgd5*$^{mCherry/+}$ and *Fgd5*$^{+/+}$ mice robustly reconstituted 2° hosts showing comparable repopulating activity, and no differences in lineage output (Fig. 3 B). Thus, inactivation of one *Fgd5* allele has no adverse consequence on the long-term repopulating or self-renewal potential of HSCs.

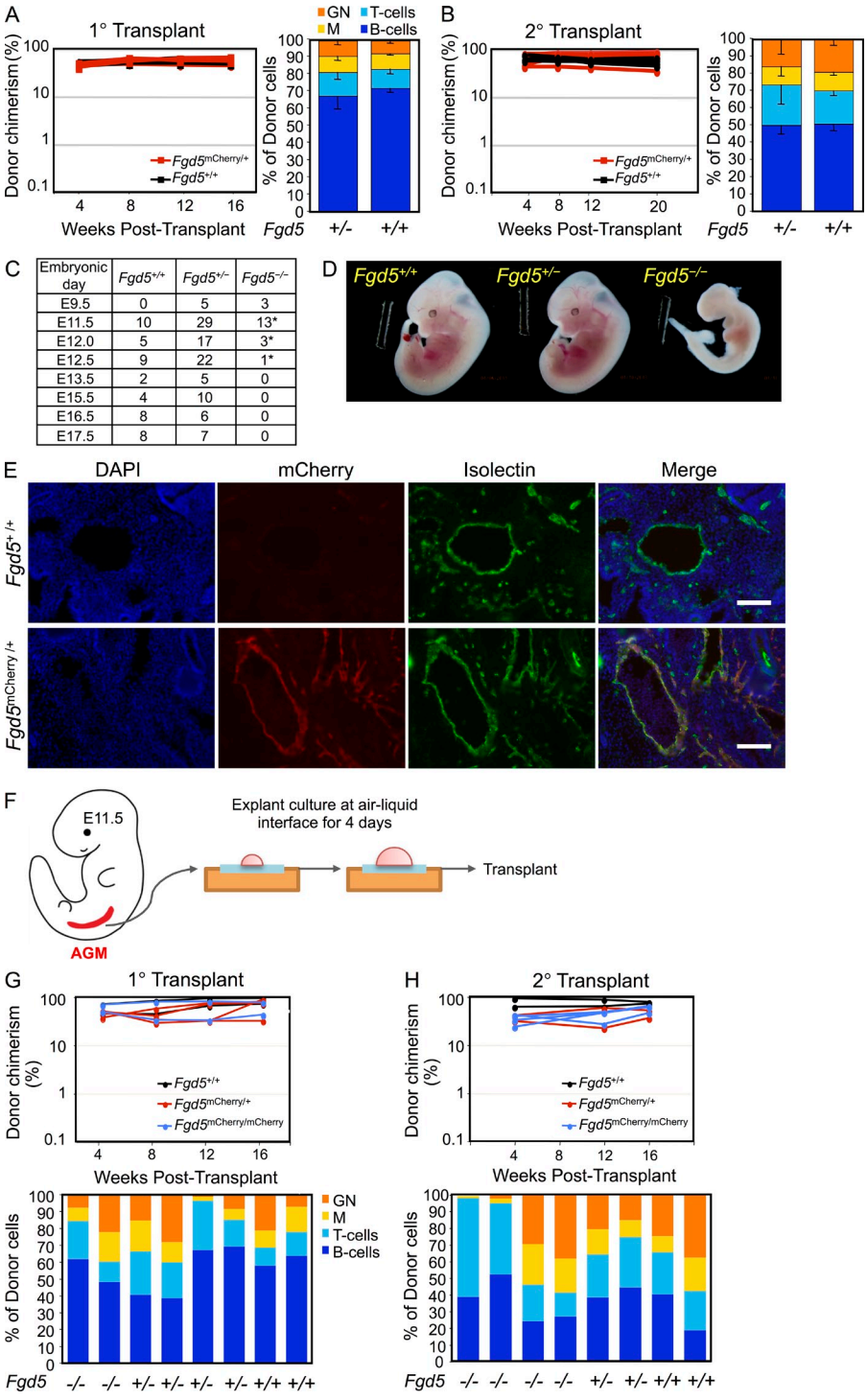

Figure 3. *Fgd5* is required for embryonic development but is dispensable for definitive HSC formation and function. (A) Primary (1°) and (B) secondary (2°) transplantation of whole BM cells from *Fgd5*$^{mCherry/+}$ (red) and *Fgd5*$^{+/+}$ (black) mice showing total donor reconstitution (left) over the time course of transplantation and lineage breakdown of donor cells at 16 (1°) and 20 (2°) wk after transplant (right). Number of recipients: $n = 9$ and 5 (*Fgd5*$^{mCherry/+}$) and 8 and 4 (*Fgd5*$^{+/+}$) for 1° and 2° transplants, respectively, error bars indicate SD. (C) Table summarizing genotypes *Fgd5*$^{+/+}$ (WT), *Fgd5*$^{mCherry/+}$ (Het), and *Fgd5*$^{mCherry/mCherry}$ (null) and number of embryos recovered at indicated time points of embryonic development from *Fgd5*$^{+/mCherry}$ X *Fgd5*$^{+/mCherry}$ crosses. * indicates the presence of one or more morphologically abnormal embryos. (D) Dissecting microscope images of E12.0 embryos derived from *Fgd5*$^{mCherry/+}$ X *Fgd5*$^{mCherry/+}$ timed matings showing genotype and gross morphology of the embryos. (E) Histological sections showing the mCherry signal at the aorta gonad mesonephros (AGM) region of E11.5 embryos derived from *Fgd5*$^{mCherry/+}$ X *Fgd5*$^{+/+}$ timed matings stained with FITC-Isolectin (for endothelial cells) and counterstained with DAPI. Figure shows separate channels and overlay of a representative *Fgd5*$^{+/+}$ (top) and *Fgd5*$^{mCherry/+}$ (bottom) embryos (bars, 100 µm). (F) Schematic of experimental strategy for AGM-explants and transplantation. (G) Primary (1°) and (H) secondary (2°) transplantation of AGM explants derived from *Fgd5*$^{+/+}$ (black), *Fgd5*$^{mCherry/+}$ (red), and *Fgd*$^{mCherry/mCherry}$ (blue) embryos showing total donor reconstitution (top) over the time course of transplantation and lineage breakdown of donor cells in individual recipient at 16 wk after transplant (bottom). Granulocytes (GN), macrophage/monocytes (M), B cells, and T cells are indicated by color. Data are shown for all embryos transplanted in primary and secondary recipients.

We next sought to determine if *Fgd5* nullizygosity would have an impact on HSC function. To address this, we set *Fgd5*$^{mCherry/+}$ X *Fgd5*$^{mCherry/+}$ crosses but were unable to obtain any viable *Fgd5*$^{mCherry/mCherry}$ offspring, indicating that ablation of *Fgd5* is lethal for embryos. We examined the requirement for *Fdg5* during embryonic development and found that whereas no *Fgd5*$^{mCherry/mCherry}$ embryos could be identified at embryonic day 13.5 (E13.5) or later, null embryos could be obtained at Mendelian numbers at E11.5 (Fig. 3 C). Gross examination and genotyping of embryos from timed matings showed that although many *Fgd5*-null embryos appeared morphologically normal at E11.5, the presence of resorbed embryos and *Fgd5*$^{mCherry/mCherry}$ embryos with clear morphological abnormalities at E12.0 indicate that most *Fgd5*-null embryos die around E11.5–E12.0 (Fig. 3, C and D). Histological examination of the aorta-gonad mesonephros (AGM) region of E11.5 control and morphologically normal *Fgd5*$^{mCherry/+}$ embryos revealed that all endothelial cells, including the aorta, were mCherry$^+$ (Fig. 3 E), which is consistent with the previously reported pan-endothelial cell expression of *Fgd5* in developing embryos (Cheng et al., 2012). Because the timing of death (E11.5–E12.0) is shortly after the developmental time point at which definitive HSCs first emerge in the embryo at the AGM region (Dzierzak and Speck, 2008), the possibility that definitive hematopoiesis may be defective or impaired in absence of FGD5 was raised. To test this possibility directly, we dissected the AGM region of E11.5 embryos derived from *Fgd5*$^{mCherry/+}$ X *Fgd5*$^{mCherry/+}$ crosses and cultured them for 4 d at an air/liquid interface using an adapted protocol (Medvinsky and Dzierzak, 1996; Taoudi et al., 2008), and then competitively transplanted all the cells from the AGM explants into irradiated recipients (Fig. 3 F). These experiments showed that although there was some variability in lineage output, as might be expected with this protocol, AGM explants arising from *Fgd5*$^{+/+}$, *Fgd5*$^{mCherry/+}$, or *Fgd5*$^{mCherry/mCherry}$ embryos all gave rise to HSCs capable of long-term multilineage reconstitution in 1° recipients (Fig. 3 G). To further test the functional capacity of the *Fgd5*-deficient HSCs, 2×10^6 BM cells from the 1° hosts were serially transplanted into 2° recipients. These experiments showed that AGM-derived HSCs of all *Fgd5* genotypes were able to give rise to long-term, multilineage reconstitution in 2° hosts (Fig. 3 H).

Collectively, these results indicate that *Fgd5* is required for embryonic development, but is not required for the generation of definitive HSCs, and further that loss of one or both *Fgd5* alleles does not impair the long-term self-renewal or multilineage differentiation potential of HSCs in serial transplantation assays.

It is also important to note that although the targeting of *Clec1a* or *Sult1a1* did not faithfully label HSCs, we were nonetheless able to determine that neither gene was required for embryonic development as homozygous null mice were born at Mendelian numbers and appeared phenotypically normal. Moreover, BM from mice harboring *Clec1a* or *Sult1a1* alleles functioned normally in primary transplantation assays, indicating that neither gene was required for HSC long-term repopulating activity (unpublished data).

Fgd5^{mCherry} identifies BM cells with potent hematopoietic stem cell activity

Having determined that the mCherry$^+$ BM fraction of *Fgd5*$^{mCherry/+}$ mice labels cells that express markers consistent with immunophenotypic HSCs (Fig. 2), and also that the targeted allele had no adverse effect on HSC function (Fig. 3), we next sought to test the functional activity of the labeled cells directly. We sorted defined numbers of cells based solely on mCherry positivity from the BM of *Fgd5*$^{mCherry/+}$ mice (CD45.2), and competitively transplanted them into lethally irradiated congenic recipients (CD45.1). We also sorted immunophenotypic HSCs (LSKCD150$^+$CD48$^-$, hereafter referred to as HSC^{Slam}) and competitively transplanted these in parallel. In a series of independent experiments, mCherry$^+$ cells, and HSC^{Slam} were transplanted at 200, 120, 40, 20, or 5 cells per recipient, and peripheral blood reconstitution was monitored for 16 wk (Fig. 4, A–E). At all transplant doses, the mCherry$^+$ cells and HSC^{Slam} gave rise to long-term donor chimerism that was statistically comparable (Fig. 4 F). In each of the 200, 120, 40, and 20 cell transplants, all recipient mice transplanted with either mCherry$^+$ cells or HSC^{Slam} showed donor-derived multilineage reconstitution 16 wk after transplant, whereas at the 5-cell dose, 11/13, and 8/13 recipients were multilineage reconstituted when mCherry$^+$ cells or HSC^{Slam} were transplanted, respectively (Fig. 4, A–E). These results demonstrate that the mCherry$^+$ fraction of *Fgd5*$^{mCherry/+}$ BM is highly enriched with potent repopulating activity that is functionally comparable, on a per cell basis, to HSCs sorted by rigorous immunophenotypic markers.

In addition to the ability to give rise to long-term multilineage reconstitution in 1° transplant recipients, HSCs are most rigorously experimentally defined by their ability to sustain activity during serial transplantation. To address this, we again isolated mCherry$^+$ cells or HSC^{Slam} from *Fgd5*$^{mCherry/+}$ or *Fgd5*$^{+/+}$ mice (CD45.2), respectively, and competitively transplanted 250 cells of each into irradiated congenic (CD45.1) recipients. Analysis of 1° recipients revealed, as before, that the mCherry$^+$ cells and HSC^{Slam} performed comparably (Fig. 5 A). 21 wk after transplant, 2×10^6 BM cells derived from the 1° recipients were transplanted into 2° hosts (CD45.1). Throughout the 28-wk-long experiment, all 2° hosts showed donor-derived multilineage reconstitution (Fig. 5 B). 31 wk after transplant, BM cells were harvested from the 2° hosts and 5×10^6 cells were transplanted into tertiary (3°) recipients (CD45.1). As we had observed in the 2° hosts, both the mCherry$^+$ donor cells and HSC^{Slam} controls continued to show potent long-term multilineage repopulating activity in all of the 3° recipients (Fig. 5, C and D). These experiments demonstrate that the mCherry$^+$ fraction of *Fgd5*$^{mCherry/+}$ BM contains potent multilineage repopulating potential, and extensive self-renewal potential in vivo.

We next analyzed the BM reconstitution of recipients that had been transplanted with either mCherry$^+$ cells or HSC^{Slam}.

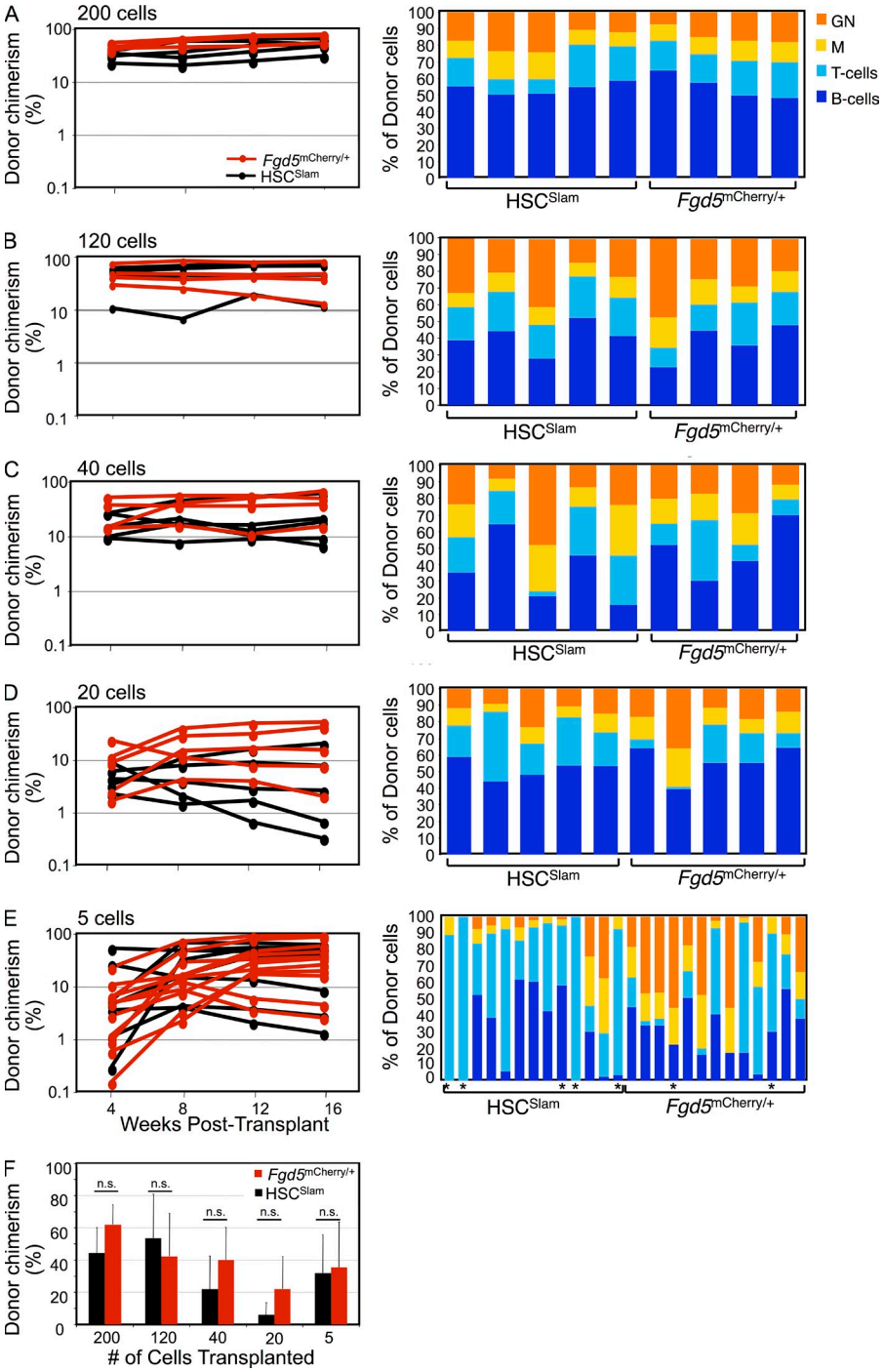

Figure 4. *Fgd5*^{mCherry} identifies cells with potent HSC activity. (A–E) Transplantation of 200 (A), 120 (B), 40 (C), 20 (D), or 5 (E) mCherry$^+$ cells from *Fgd5*$^{mCherry/+}$ mice (red) or control LSKCD48$^-$CD150$^+$-sorted HSCs (HSC^{Slam}) from wild-type mice (black) showing total donor reconstitution (left) over the time course of transplantation, and lineage breakdown of donor cells in individual recipient mice at 16-wk after transplant (right). Asterisks (*) in E indicate mice that were not multilineage reconstituted at the 5-cell transplant dose. Granulocytes (GN), macrophage/monocytes (M), B cells, and T cells are indicated by color. (F) Mean total donor chimerism of each of the experiments shown in A–E. Error bars indicate SD, $P > 0.05$, by Student's *t* test.

Similar to the chimerism observed in the peripheral blood (Fig. 4), the BM was robustly reconstituted with CD45.2 donor-derived cells regardless of whether mCherry$^+$ cells or HSC^{Slam} had been transplanted (Fig. 6). Co-staining the BM with a panel of markers showed, as we had observed in the steady state (Fig. 2), that the mCherry$^+$ signal was restricted to the immunophenotypic HSC (LSKflk2$^-$CD34$^-$) compartment, with only a minor fraction of the LSK multipotent progenitors expressing lower levels of labeling (Fig. 6 C). These results show that the mCherry$^+$ cells are able to self-renew to give rise to immunophenotypic HSCs in vivo and, further, that the near exclusive labeling of HSCs observed in the BM of *Fgd5*$^{mCherry/+}$ mice is faithfully maintained even after the extensive challenge of primary transplantation.

All HSC activity resides within the mCherry$^+$ fraction of *Fgd5*$^{mCherry/+}$ BM

We next sought to determine if all HSC activity was confined to the mCherry$^+$ fraction of the *Fgd5*$^{mCherry/+}$ BM. To address this, we sorted the BM of *Fgd5*$^{mCherry/+}$ mice into

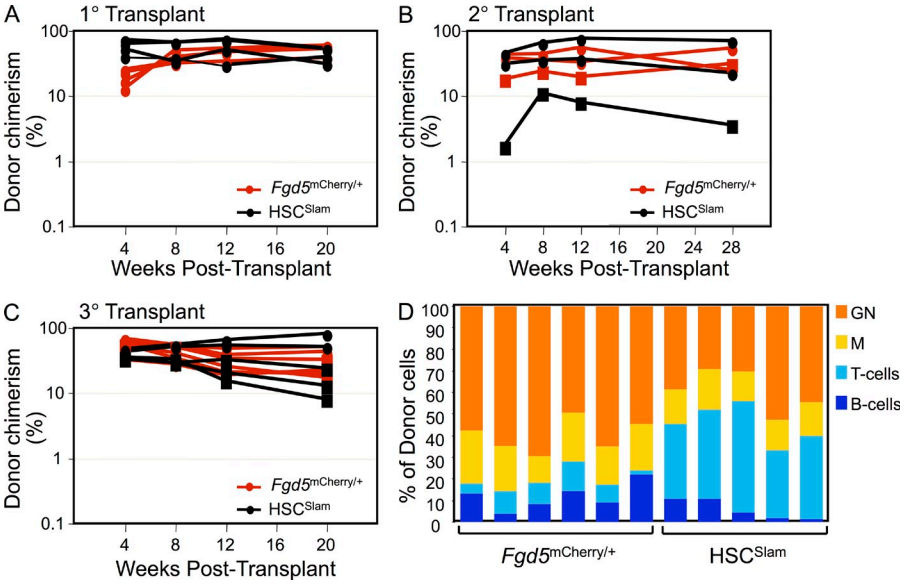

Figure 5. *Fgd5*^{mCherry}–labeled HSCs have extensive self-renewal and repopulating potential. (A) Primary (1°) transplantation of 250 mCherry$^+$ cells from *Fgd5*$^{mCherry/+}$ mice (red), or 250 control LSKCD48$^-$CD150$^+$-sorted HSCs (HSC^{Slam}) from wild-type mice (black) showing total donor reconstitution over the time course of transplantation (n = 4 recipients per group). (B) Secondary (2°; n = 3 recipients per group) and (C) tertiary (3°) transplantation (number of recipients n = 6 [*Fgd5*$^{mCherry/+}$] and 5 [HSC^{Slam}]) of whole BM cells from the 1° recipients described in A showing total donor reconstitution over the time course of transplantation. (D) Lineage breakdown of donor cells at individual recipients at 20 wk after transplant from the 3° transplants. Granulocytes (GN), macrophage/monocytes (M), B cells, and T cells are indicated by color.

mCherry$^+$ and mCherry$^-$ fractions, and competitively transplanted either 100 or 100,000 cells, respectively, into irradiated recipients in two independent experiments (Fig. 7, A–C). As we had previously observed (Figs. 4–5), the 100-mCherry$^+$ cell transplants all yielded robust long-term, multilineage reconstitution in both experiments (Fig. 7, B–D). In contrast, the 100,000-mCherry$^-$ cell transplants yielded only short-term reconstitution that gradually diminished to very low levels at later time-points (Fig. 7, B and C). Peripheral blood analysis of the few remaining mCherry$^-$ donor-derived cells at 16-wk (experiment #1) or 24-wk (experiment #2) after transplant revealed that virtually all were B and T cells, which

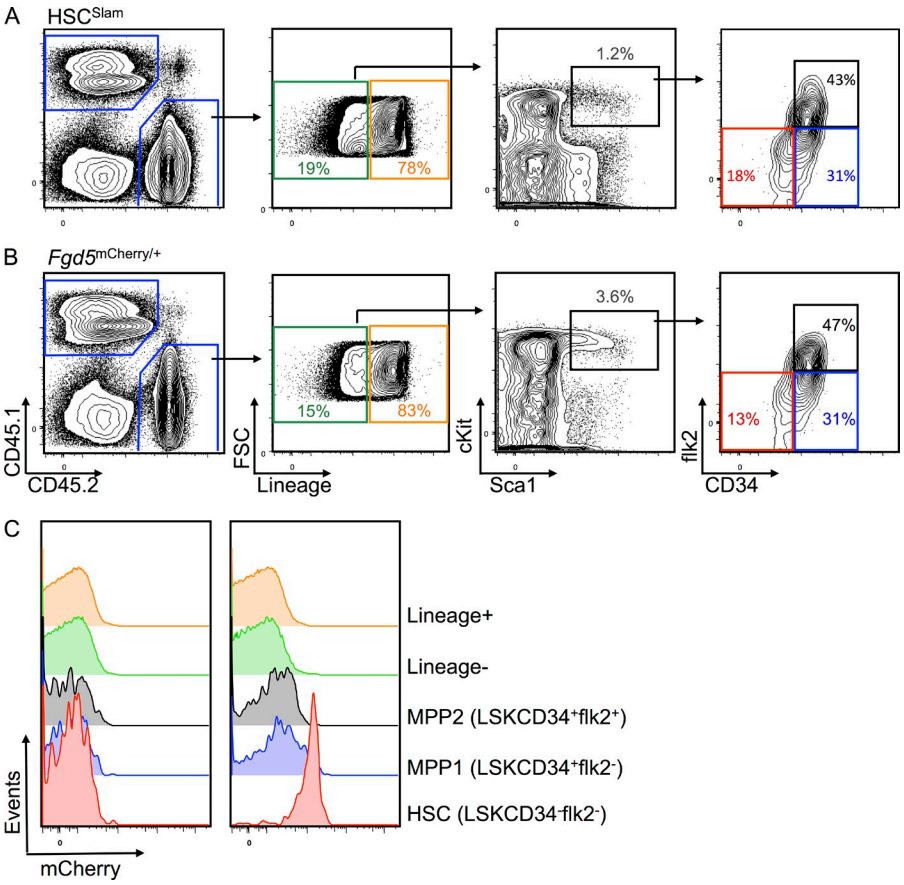

Figure 6. Labeling of HSCs by *Fgd5*$^{mCherry/+}$ is retained after transplantation. (A and B) BM analysis of recipient mice transplanted with 120 LSKCD48$^-$CD150$^+$ HSCs (HSC^{Slam}) from wild-type mice (A) or 120 mCherry$^+$ cells from *Fgd5*^{mCherry} mice (B), analyzed 8 mo after transplant showing donor-derived (CD45.2) chimerism and contribution to BM compartments revealed by co-staining with antibodies against lineage, c-Kit, Sca1, flk2, and CD34. (C) Histograms showing mCherry signal in the indicated cell fractions from the BM of recipient mice transplanted with 120 HSC^{Slam} cells from wild-type mice (left) or 120 mCherry$^+$ cells from *Fgd5*^{mCherry} mice 8 mo after transplant. Representative data from n = 4 mice per group.

can be long-lived (Fig. 7 D). Importantly, although the mCherry$^+$ cell transplants all gave rise to sustained, high levels of granulocyte chimerism indicating robust, ongoing HSC activity (Bhattacharya et al., 2006; Bryder et al., 2006), granulocyte reconstitution was progressively extinguished in the recipients transplanted with the mCherry$^-$ fraction indicating an absence of HSC activity (Fig. 7, E and F). The sole exception to this was one of the recipients of 100,000 mCherry$^-$ cells in experiment #1 showed very low donor-derived granulocyte reconstitution 16 wk after transplant (Fig. 7 E). Although we cannot formally exclude the possibility that HSC activity resides in the mCherry$^-$ fraction of the BM at very low frequency, the fact that only 1 out of 10 independent recipients transplanted with 100,000 mCherry$^-$ cells showed minor granulocyte reconstitution 16 wk after transplant, indicates that most, if not all, of HSC activity resides in the mCherry$^+$ fraction of the *Fgd5*$^{mCherry/+}$ mice.

Pan-endothelial Fgd5 expression in adult BM, and inducible HSC-specific Cre-mediated deletion revealed by next generation *Fgd5* mice

Our functional data to this point indicates that *Fgd5* would be an ideal locus for the construction of additional genetic tools designed to study the functional, molecular, and therapeutic

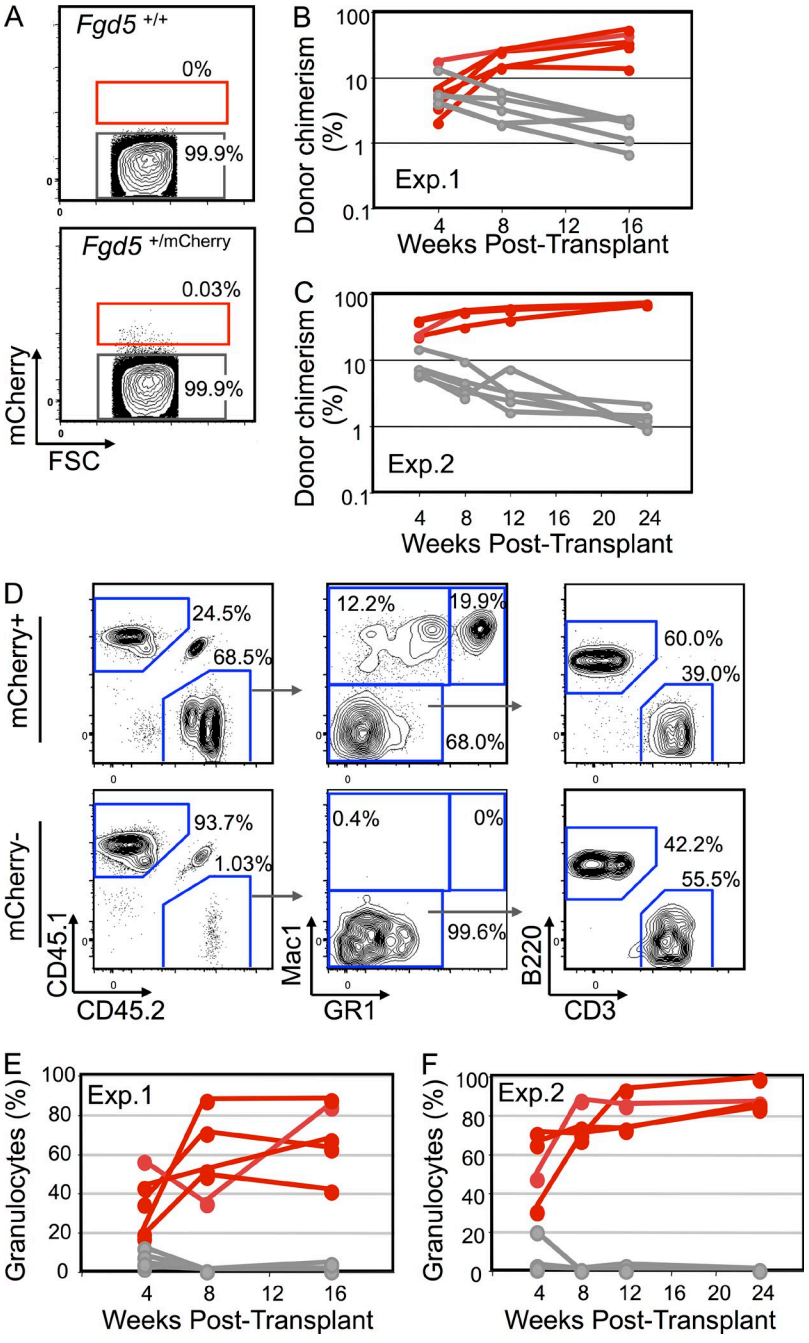

Figure 7. All HSCs are labeled by *Fgd5*^{mCherry}. (A) Gating strategy used for sorting reporter-positive and -negative fractions set using *Fgd5*$^{+/+}$ (top) and *Fgd5*$^{mCherry/+}$ (bottom) mice. (B and C) Transplantation of 100 mCherry$^+$ (red) or 100,000 mCherry$^-$ (gray) cells from *Fgd5*$^{mCherry/+}$ mice showing total donor reconstitution over the time course of transplantation in experiment 1 (B) and experiment 2 (C). (D) Peripheral blood analysis of representative recipients from experiment 2 showing donor reconstitution (CD45.2) and contribution to granulocytes (Mac1$^+$Gr1$^+$), macrophages/monocytes (Mac1$^+$Gr1$^-$), B cells (Mac1$^-$, B220$^+$CD3$^-$) and T cells (Mac1$^+$, B220-CD3$^+$) analyzed 24-wk after transplant. (E and F) Peripheral blood analysis showing granulocyte chimerism plotted against the time course of transplantation in experiments 1 (E) and 2 (F). $n = 5$ per group in experiment 1; $n = 4$ (*Fgd5*$^{mCherry/+}$); $n = 5$ (*Fgd5*$^{+/+}$) in experiment 2.

properties of HSCs. To expand the repertoire of HSC-specific genetic resources we generated two additional strains by targeting the *Fgd5* locus in ES cells. With the intent of generating a brighter *Fgd5* reporter that could be detected using 488-nm lasers common to most flow cytometers and FACS machines, we knocked-in tandem ZsGreen cassettes separated by a 2A peptide into the *Fgd5* locus. Similar to the $Fgd5^{mCherry/+}$ mice (Fig. 2), the vast majority of ZsGreen$^+$ cells were lineage (lin$^-$) and CD48$^-$, and c-Kit$^+$, Sca1$^+$, and CD150$^+$ (Fig. 8 A). Consistent with the brighter expression of the $Fgd5^{ZsGr•ZsGr/+}$ reporter, and also with the expression of *Fgd5* transcript observed in multipotent progenitor subsets (Fig. 1 C), LSKCD48$^-$CD150$^-$ (MFI 6,031) and to a lesser extent, LSKCD48$^+$CD150$^-$ (MFI 1,566) progenitor subsets, expressed *Fgd5*-ZsGreen signal, albeit at lower levels than observed in LSKCD48$^-$CD150$^+$ HSCs (MFI 11,343; unpublished data). *Fgd5* reporter signal was detected in all HSC subtypes fractionated by differential CD150 expression in young (4 mo) and mid-aged (14 mo) mice (Fig. 8, B and C; Beerman et al., 2010; Morita et al., 2010). Interestingly, CD150^{hi} HSCs, which are believed to be the most primitive HSC subset (Beerman et al., 2010; Morita et al., 2010), showed the highest mean fluorescence intensity of *Fgd5* reporter signal, followed by CD150^{lo} HSCs and CD150^{neg} HSCs (Fig. 8 C), suggesting that the intensity of *Fgd5* reporter expression tracks with HSC potency, and further that the *Fgd5* reporter faithfully tracks the changes in the HSC population during aging.

Using this strain we next sought to examine *Fgd5* expression in the adult BM using laser-scanning cytometry (Nombela-Arrieta et al., 2013). Consistent with previous studies suggesting pan-endothelial expression of *Fgd5* (Cheng et al., 2012; Kurogane et al., 2012), all blood vessels in the adult BM expressed high levels of the *Fgd5* reporter (Fig. 8 D and Video 1).

The most widely used genetic resources for investigating gene function in HSCs via loss-of-function approaches are the *Mx1*-Cre (Kühn et al., 1995) and *Vav1*-Cre (de Boer et al., 2003) strains. Although both strains are robust, they both have limitations for specifically studying gene function in HSCs as both are pan-hematopoietic. Moreover, *Vav1*-Cre is noninducible, thus precluding temporal control of gene deletion, and although *Mx1*-Cre is inducible, its induction by the synthetic double-stranded RNA polyinosinic-polycytidylic acid (polyI:polyC) elicits a systemic interferon response that is known to activate and drive HSCs into cycle (Baldridge et al., 2010; Essers et al., 2009) potentially confounding interpretations using this strain, particularly in regard to HSC cell cycle status and regulation of quiescence. To circumvent these issues, we targeted an inducible CreERT2 cassette along with a ZsGreen reporter cassette into the *Fgd5* locus in ES cells to derive $Fgd5^{ZsGr•CreERT2/+}$ mice. These mice were then crossed to mice bearing a floxed-stop dTomato reporter allele at the Rosa26 locus. After tamoxifen induction, we examined the specificity and efficacy of Cre-mediated deletion. These experiments showed that dTomato expression after Cre-mediated excision of floxed-stop cassette was highly restricted to ZsGreen$^+$ LSKCD150$^+$ HSCs (Fig. 9 A), with essentially no dTomato expression detected in other hematopoietic compartments (Fig. 9 B).

DISCUSSION

In this study, we set out to identify genes with restricted expression in the HSC compartment of the murine BM, and then target the endogenous loci of several identified genes in mouse ES cells to generate reporter knock-in/knock-out alleles. Mice bearing such alleles could potentially be used to identify HSCs by single-color fluorescence without the need for immunostaining, which could have great utility for addressing outstanding questions related to HSC biology. At the same time, our knock-in/knock-out approach would allow us to examine the requirement of the targeted genes for HSC development and function. To achieve these goals, we used a microarray approach in which we compared the expression profiles of highly purified HSCs to that of 36 downstream progenitor and effector cell types. Previous studies using related approaches have been successful in identifying genes that function in HSCs or in downstream populations (Ivanova et al., 2002; Park et al., 2002; Forsberg et al., 2005; Kiel et al., 2005a; Shojaei et al., 2005; Balazs et al., 2006; Luckey et al., 2006; Chambers et al., 2007a,b; Seita et al., 2012; Gazit et al., 2013), as well as genes whose products serve as antigens that have been used to facilitate identification of HSCs such as *Esam* (Forsberg et al., 2005), the Slam code (CD150, CD48, and CD244; Kiel et al., 2005a), and *Procr/CD201* (Balazs et al., 2006). Mindful of the fact that HSCs share several functional attributes with their proximal multipotent progenitor progeny, and also, to a lesser degree, with downstream oligopotent and lineage-restricted progenitors, we included such populations in our microarray screen reasoning that this would allow us to more precisely identify genes with HSC-restricted expression. With this said, it must be recognized that identifying a gene as "specific" to any cell type is ultimately limited by the spectrum and comprehensiveness of the samples studied. Bearing this potential caveat in mind, using the hematopoietic database assembled for this study, we were able to identify 235 annotated genes with highly restricted expression in HSCs, many of which have not been previously studied in the context of HSC biology.

To assess the potential functional role that such novel identified genes might play in HSCs, and to increase the likelihood of identifying a genomic locus that upon targeting would lead to faithful HSC labeling, we focused on three genes with highly HSC-restricted expression. The knock-in/knock-out targeting strategy we used allowed us to determine that neither *Clec1a* nor *Sult1a1* are required for normal mammalian development, and both appeared to be dispensable for HSC function in transplantation experiments (unpublished data). In contrast, whereas *Fgd5* heterozygotes developed normally and showed no deficit in HSC function, *Fgd5* nullizygosity was embryonic lethal at mid-gestation, indicating a critical, nonredundant function for FGD5 during development. Recent studies have shown that *Fgd5* expression

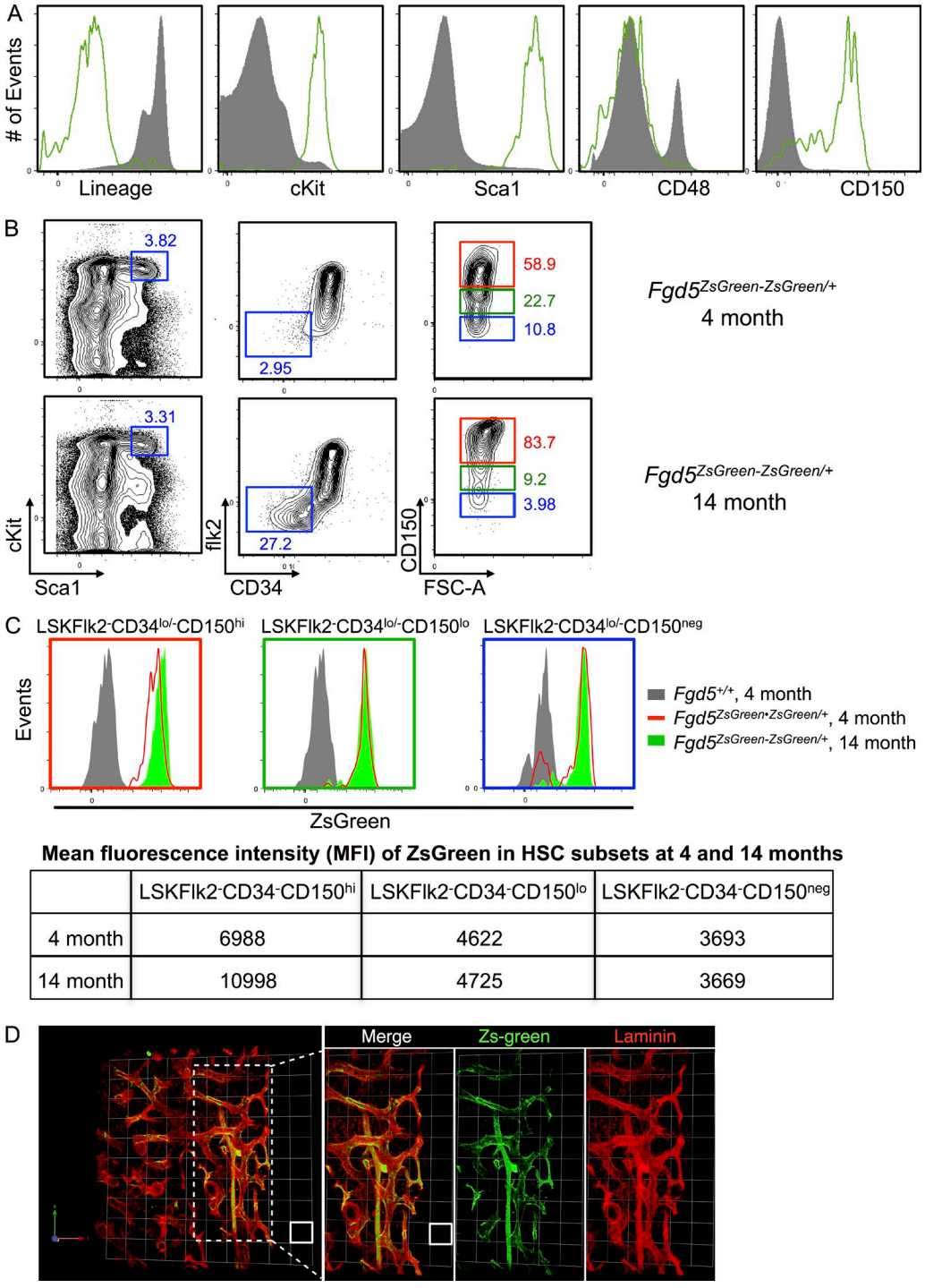

Mean fluorescence intensity (MFI) of ZsGreen in HSC subsets at 4 and 14 months

	LSKFlk2$^-$CD34$^-$CD150^{hi}	LSKFlk2$^-$CD34$^-$CD150^{lo}	LSKFlk2$^-$CD34$^-$CD150^{neg}
4 month	6988	4622	3693
14 month	10998	4725	3669

Figure 8. Fgd5$^{ZsGreen•ZsGreen/+}$ reporter expression marks all HSC subtypes and also endothelial cells in the BM. (A) BM ZsGreen$^+$ (green histograms) and ZsGreen$^-$ (gray histograms) cells of *Fgd5*$^{ZsGreen•ZsGreen/+}$ mice co-stained and gated through lineage (Ter119, Mac-1, Gr-1, B220, CD3, CD4, CD8, and IL7Rα), c-Kit, Sca1, CD48, and CD150 (n = 5 or more). (B) Sub-fractionation of LKSFlk2$^-$CD34$^{-/low}$ into CD150^{hi} (red gates), CD150^{lo} (green gates), and CD150^{neg} (blue gates) HSC subtypes from young (4 mo) and mid-aged (14 mo) Fgd5$^{+/+}$ and Fgd5$^{ZsGreen•ZsGreen/+}$ mice. (C) Histograms showing ZsGreen expression of each of the indicated HSC subtypes from the mice shown in B. MFI of each of the indicated HSC subtypes is shown (bottom). A minimum of n = 3 mice for each stained were analyzed with the exception of 14-mo-old mouse (n = 1). (D) Adult femoral BM cavity microvascular network based on 3D reconstruction of a series of confocal images showing arterial and sinusoidal microvessels (stained with Laminin in red) and Fgd5$^{Zsgreen•ZsGreen/+}$ reporter expression (green). Projection depth 54 µm. Grid squares (white box) are 51.3 µm × 51.3 µm (left) and 42.9 µm × 42.9 µm (right).

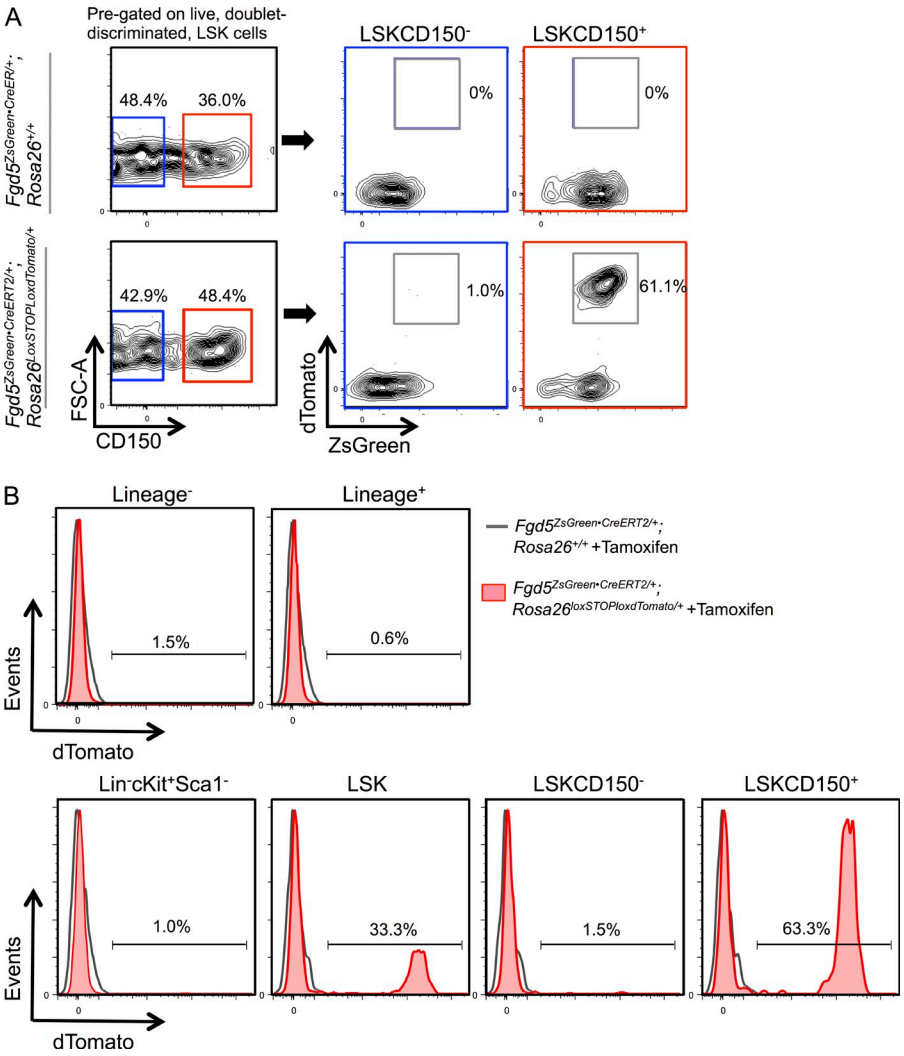

Figure 9. Tamoxifen induced Cre activity in *Fgd5*$^{ZsGreen•CreERT2/+}$ mice exclusively targets CD150$^+$ HSCs. (A) Flow plots of tamoxifen-treated *Fgd5*$^{ZsGreen•CreERT2/+}$:*Rosa26*$^{+/+}$ and *Fgd5*$^{ZsGreen•CreERT2/+}$:*Rosa26*$^{LoxSTOPLoxdTomato/+}$ mice showing primitive LSK compartment subfractionated into CD150- and CD150$^+$ population (left), with each population then gated through ZsGreen and dTomato (right). (B) Cre-mediated dTomato expression in control *Fgd5*$^{ZsGreen•CreERT2/+}$; *Rosa26*$^{+/+}$ *and* experimental *Fgd5*$^{ZsGreen•CreERT2/+}$; *Rosa26*$^{loxSTOPloxdTomato/+}$ mice upon tamoxifen induction shown in the indicated BM populations including Lineage$^-$, Lineage$^+$, Lin$^-$cKit$^+$Sca1$^-$ (myeloid progenitors), LSKCD150$^-$ cells, LSK, and LSKCD150$^+$ HSC (n = 3 per group).

outside of the hematopoietic system is predominantly restricted to endothelial cells in developing and adult mice and in zebrafish embryos (Cheng et al., 2012). *Fgd5* is also expressed in several human endothelial cell lines, where it has been suggested to play a role regulating CDC42 activity during capillary formation (Kurogane et al., 2012). The importance of *Fgd5* in endothelial cell biology was recently demonstrated in a study in which murine *Fgd5* was knocked-down by siRNA, and overexpressed, showing that FGD5 regulates vascular pruning during endothelial cell remodeling (Cheng et al., 2012). These studies raise the possibility that the embryonic lethality associated with loss of FGD5 may result from defective vasculogenesis. Consistent with this we observed robust endothelial expression of FGD5 in the developing embryo and also in adult BM. With regards to hematopoiesis, we showed that despite the midgestation lethality, *Fgd5*-nullizygosity did not impair the formation or function of definitive HSCs (Fig. 3), which retained self-renewal and multilineage differentiation potential comparable to wild-type controls.

Several previous studies have targeted a variety of loci with the intent of establishing a reporter that specifically identifies HSCs. Mice bearing a reporter for the *Gata2* transcription factor that is not specifically expressed in HSCs (Fig. S1) were found to be useful for enriching for HSC activity when sorted in combination with immunostaining for Sca1 (Suzuki et al., 2006). Similarly, although mice bearing a reporter allele at the *Abcg2* locus predominantly labeled Ter119$^+$ erythroid cells in the murine BM as expected from expression analysis (Fig. S1), HSCs could be identified when used in combination with side-population activity, and antibody staining to exclude lineage$^+$ cells (Tadjali et al., 2006). Interestingly, although *Bmi-1* is broadly expressed throughout hematopoiesis (Fig. S1), mice bearing a GFP knock-in allele at the *Bmi-1* locus, which is critical for HSC function (Park et al., 2003), were used to demonstrate that BM cells expressing the highest levels of GFP contained HSC activity when sorted in combination with additional HSC markers (Hosen et al., 2007). In an elegant study, Goyama et al. (2008) targeted the *Evi-1* locus, which is required for HSC function, by cleverly knocking-in an *Evi-1* cDNA-IRES-GFP rescue/reporter cassette, which largely rescued HSC activity (Kataoka et al., 2011). This study showed that although the majority of

cells of the primitive LSK compartment were GFP-labeled in these mice, only the GFP$^+$ fraction when sorted in combination with additional HSC markers including Lin$^-$Sca1$^+$c-kit$^+$ exhibited HSC activity (Kataoka et al., 2011). Thus, to the best of our knowledge, although several reporter mice have been developed that label hematopoietic stem and progenitor cells, the goal of establishing a reporter strain that faithfully and more specifically labels HSCs based on single-color fluorescence has not been previously achieved.

Although *Clec1a* and *Sult1a1* were identified as being among the most HSC-restricted genes from our expression screen, targeting expression reporter cassettes into the coding region of these genes did not lead to expression in the HSC compartment. Several reasons could underlie this disappointing outcome, including the possibility that targeting the loci in the manner that we did sufficiently disrupted regulatory elements necessary for expression in HSCs. In contrast to *Clec1a* and *Sult1a1*, targeting of the *Fgd5* locus yielded a reporter that almost exclusively labels HSCs in the murine BM. In addition to being essentially synonymous with a myriad of markers that are used to immunophenotypically identify HSCs (Osawa et al., 1996; Kiel et al., 2005b; Balazs et al., 2006; Bryder et al., 2006; Ooi et al., 2009), cells sorted solely on reporter signal from the *Fgd5*$^{mCherry/+}$ mice had potent HSC activity that matched the functional potential of rigorously immunopurified HSCs (Kiel et al., 2005b). We demonstrated that the *Fgd5* reporter effectively marked all HSC activity in the steady-state BM, which is remarkable in light of evidence showing that even widely used protocols that have proven very effective in identifying HSCs do not strictly identify all cells with HSC activity (Morita et al., 2006; Weksberg et al., 2008). Moreover, the demonstration that *Fgd5* reporter activity exclusively identified immunophenotypic HSCs in the BM of transplanted mice suggests that even under experimental settings requiring extensive HSC activity and self-renewal *Fgd5* reporter expression remained a powerful tool for identifying HSCs. The *Fgd5* reporter and *Fgd5-CreERT2* mice reported here represent invaluable resources for studying the pathways and mechanisms that govern the central properties of HSCs under diverse settings.

MATERIALS AND METHODS

Hematopoietic expression database. Microarray data were generated on the Affymetrix 430 2.0 platform and included previously unpublished data generated in our laboratory in addition to datasets that were curated from Gene Expression Omnibus (complete list of accession nos. available in Table S1). All datasets were subjected to quality control (QC) measures provided in the ArrayQualityMetrics package of R/Bioconductor. Datasets were normalized (gcRMA) using R/Bioconductor. To identify cell type–specific genes we applied three filters: (1) only probe sets that had expression values ≥ log 7.0 were included; (2) Ratio of expression difference for the cell type of interest to all others had to be greater than fourfold; (3) Statistical significance for the cell type of interest to all others had to be $P < 10^{-6}$ by Student's *t* test.

Gene targeting and mice. The targeting constructs were built using the W vector (provided by J. Segal and K. Rajewsky, Immune Disease Institute, Boston). Homologous arms were cloned by PCR from genomic DNA of C57BL/6 mice. Constructs were sequenced validated. ES cells (B6/3) derived from C57BL/6 mice were electroporated with linearized constructs and clones were positively selected with G418 and negatively selected by the diphtheria toxin cassette of the constructs. Clones were manually picked, expanded, and screened by Southern blot. Positive clones were expanded, validated, and injected into blastocysts, and germline transmission was confirmed. All strains used were on a C57BL/6 background including CD45.1 and CD45.2 congenic, and the Rosa26-LoxP-STOP-LoxP-tdTomato (stock# 007914) was obtained from The Jackson Laboratory. All experiments involving mice were done per institutional guidelines of The Harvard Medical School Standing Committee on Animals, with IACUC approval.

FACS analysis and cell sorting. BM mononuclear cells prepared over Histopaque 1083 (Sigma-Aldrich) were stained for 1.5 h in PBS 2 mM EDTA, 2% FBS at 4°C with combinations of the following antibodies: the lineage markers Ter119, Mac-1 (m1/70), Gr-1 (8C5), CD3 (17A2), CD4 (RM4-5), CD8 (53–6.7), B220 (RA3-6B2), and IL7Ra (A7R34); CD34 (RAM34), Flk2 (A2F10), c-kit (2B8), Sca1 (D7), CD150 (TC15-12F12.2), CD48 (HM48-1), CD201 (eBio1560), and ESAM (1G8; all from BioLegend or eBioscience). After staining, cells were washed and suspended with DAPI (1 µg/ml), and kept on ice. FACSAria II (BD) or MoFlo Astrios (Beckman Coulter) equipped with 590-nm lasers for optimal detection of the mCherry signal were used for cell sorting and analysis. Transplanted cells were double sorted for purity.

Transplantations and peripheral blood analysis. Congenic recipient mice were lethally irradiated (900 rad), and donor cells, mixed with 2×10^5 whole BM competitor cells in 200 µl PBS 2 mM EDTA, and 2% FBS, were injected into the tail vein. At the indicated time points, 2–3 drops of blood were collected from the tail and added to 150 µl Alsever's solution (Sigma-Aldrich). Blood samples were treated with 10 ml ACK solution (0.15 M NH_4Cl, 1 mM $KHCO_3$, and 0.1 mM EDTA) for 5 min at room temperature and washed two times with PBS. Leukocytes were stained with PerCP/Cy5.5-Ter119 (Ter119), PE/Cy7-Mac1 (m1/70), Fitc-Gr1 (8C5), PE-CD3 (17A2), APC/Cy7-B220 (RA3-6B2), A647-CD45.1 (A20), and PacBlue-CD45.2 (104); all from BioLegend. Cells were washed and suspended with propidium iodide (1 µg/ml) and analyzed on FACSCanto II (BD). Analysis was done using FlowJo software (Tree Star). For serial-transplants (secondary and tertiary), 2×10^6 cells whole BM cells were transferred into lethally irradiated congenic recipients.

AGM explants, culturing, and imaging. The procedure we used was based on a previously published protocol (Medvinsky and Dzierzak, 1996; Taoudi et al., 2008). In brief, the aorta-gonad-mesonephros (AGM) of E11.5 embryos (CD45.2) were individually dissected (excluding somites) and cultured at the air-liquid interface on Durapore 0.65-µm filters (Millipore) suspended on IMDM media containing 20% serum and 100 ng/ml SCF, IL-3, and Flt3L (PeproTech). After 4 d, cells were dissociated with Collagenase I (Worthington), filtered, and mixed with whole BM competitor cells (CD45.1) and transplanted into lethally irradiated congenic recipients (CD45.1). For microscopic visualization of the AGM region, E11.5 embryos from *Fgd5*$^{mCherry/+}$ x *Fgd5*$^{mCherry/+}$ timed matings were fixed in 2% PFA for 30 min, equilibrated in 30% sucrose, embedded in OCT, and cryosectioned, followed by staining with FITC-conjugated Isolectin and DAPI. Images were taken using a Ti-E microscope (Nikon).

3D immunohistology of BM. Thick femoral bone slices from *Fgd5*$^{ZsGreen•ZsGreen/+}$ mice were generated as previously described (Nombela-Arrieta et al., 2013). BM slices were blocked overnight in 0.2% PBS, 1% Triton, and 10% BSA and stained with rabbit anti-laminin (Sigma-Aldrich) for 2 d in blocking solution, washed overnight in PBS, and stained for 2 d with DyLight549 donkey anti–rabbit IgG (Jackson ImmunoResearch Laboratories). Whole-mount stained slices were washed in PBS and incubated overnight in FocusClear (CelExplorer Laboratory). For observation under the confocal microscope, BM slices were mounted in glass slides embedded in FocusClear. Confocal microscopy was performed with a LSM700 system (Carl Zeiss). Image stacks were rendered into 3D volumes using Volocity Software (Improvision) and exported to Photoshop (Adobe Inc.) for processing.

Tamoxifen treatment of mice. Tamoxifen was purchased from Sigma-Aldrich and suspended at 200 mg/ml in ethanol and mixed with sunflower oil to a final concentration of 10 mg/ml (10% ethanol). Tamoxifen was administered by intraperitoneal injection to 8–12-wk-old mice at 100 mg/kg body weight for 5 consecutive days. 2 d after tamoxifen treatment, the mice were sacrificed and analyzed for expression of dTomato in conjunction with immunostaining to reveal diverse hematopoietic populations.

Microarray data. All gene expression datasets used in this study are available at the Gene Expression Omnibus accession no. GSE56952.

Online supplemental material. Fig. S1 shows relative expression of all 323 probe sets and corresponding genes identified as HSC-specific in our dataset. Video 1 shows 3D reconstruction of the microvascular network of femoral BM. Table S1 lists cell types and microarrays used in this study. Table S2 is a list of genes identified as cell type specific in our study. Online supplemental materials are available at http://www.jem.org/cgi/content/full/jem.20130428/DC1.

We wish to thank Trista North, Christophe Bock, Isabel Beerman, Jane Segal, and Dvora Ghitza for expertise, input and assistance and Natasha Barteneva, Ken Ketman, John C. Tigges, and Vasilis Toxavidis for flow cytometry expertise.

R. Gazit was supported by a JCF Machiah post-doctoral fellowship. This work was supported by the National Institutes of Health grants RO1HL107630 (D.J. Rossi) and UO1DK072473-01 (D.J. Rossi), grants from GlaxoSmithKline (D.J. Rossi), The Leona M. and Harry B. Helmsley Charitable Trust (D.J. Rossi), the New York Stem Cell Foundation (D.J. Rossi), and the Harvard Stem Cell Institute (D.J. Rossi). D.J. Rossi is a New York Stem Cell Foundation Robertson Investigator.

The authors declare no competing financial interests.

Submitted: 27 February 2013
Accepted: 14 May 2014

REFERENCES

Balazs, A.B., A.J. Fabian, C.T. Esmon, and R.C. Mulligan. 2006. Endothelial protein C receptor (CD201) explicitly identifies hematopoietic stem cells in murine bone marrow. *Blood*. 107:2317–2321. http://dx.doi.org/10.1182/blood-2005-06-2249

Baldridge, M.T., K.Y. King, N.C. Boles, D.C. Weksberg, and M.A. Goodell. 2010. Quiescent haematopoietic stem cells are activated by IFN-gamma in response to chronic infection. *Nature*. 465:793–797. http://dx.doi.org/10.1038/nature09135

Barker, N., J.H. van Es, J. Kuipers, P. Kujala, M. van den Born, M. Cozijnsen, A. Haegebarth, J. Korving, H. Begthel, P.J. Peters, and H. Clevers. 2007. Identification of stem cells in small intestine and colon by marker gene Lgr5. *Nature*. 449:1003–1007. http://dx.doi.org/10.1038/nature06196

Becker, A.J., E.A. McCULLOCH, and J.E. Till. 1963. Cytological demonstration of the clonal nature of spleen colonies derived from transplanted mouse marrow cells. *Nature*. 197:452–454. http://dx.doi.org/10.1038/197452a0

Beerman, I., D. Bhattacharya, S. Zandi, M. Sigvardsson, I.L. Weissman, D. Bryder, and D.J. Rossi. 2010. Functionally distinct hematopoietic stem cells modulate hematopoietic lineage potential during aging by a mechanism of clonal expansion. *Proc. Natl. Acad. Sci. USA*. 107:5465–5470. http://dx.doi.org/10.1073/pnas.1000834107

Bertoncello, I., G.S. Hodgson, and T.R. Bradley. 1985. Multiparameter analysis of transplantable hemopoietic stem cells: I. The separation and enrichment of stem cells homing to marrow and spleen on the basis of rhodamine-123 fluorescence. *Exp. Hematol*. 13:999–1006.

Bhattacharya, D., D.J. Rossi, D. Bryder, and I.L. Weissman. 2006. Purified hematopoietic stem cell engraftment of rare niches corrects severe lymphoid deficiencies without host conditioning. *J. Exp. Med*. 203:73–85. http://dx.doi.org/10.1084/jem.20051714

Bryder, D., D.J. Rossi, and I.L. Weissman. 2006. Hematopoietic stem cells: the paradigmatic tissue-specific stem cell. *Am. J. Pathol*. 169:338–346. http://dx.doi.org/10.2353/ajpath.2006.060312

Chambers, S.M., N.C. Boles, K.Y. Lin, M.P. Tierney, T.V. Bowman, S.B. Bradfute, A.J. Chen, A.A. Merchant, O. Sirin, D.C. Weksberg, et al. 2007a. Hematopoietic fingerprints: an expression database of stem cells and their progeny. *Cell Stem Cell*. 1:578–591. http://dx.doi.org/10.1016/j.stem.2007.10.003

Chambers, S.M., C.A. Shaw, C. Gatza, C.J. Fisk, L.A. Donehower, and M.A. Goodell. 2007b. Aging hematopoietic stem cells decline in function and exhibit epigenetic dysregulation. *PLoS Biol*. 5:e201. http://dx.doi.org/10.1371/journal.pbio.0050201

Chen, C.Z., M. Li, D. de Graaf, S. Monti, B. Göttgens, M.J. Sanchez, E.S. Lander, T.R. Golub, A.R. Green, and H.F. Lodish. 2002. Identification of endoglin as a functional marker that defines long-term repopulating hematopoietic stem cells. *Proc. Natl. Acad. Sci. USA*. 99:15468–15473. http://dx.doi.org/10.1073/pnas.202614899

Cheng, C., R. Haasdijk, D. Tempel, E.H. van de Kamp, R. Herpers, F. Bos, W.K. Den Dekker, L.A. Blonden, R. de Jong, P.E. Bürgisser, et al. 2012. Endothelial cell-specific FGD5 involvement in vascular pruning defines neovessel fate in mice. *Circulation*. 125:3142–3158. http://dx.doi.org/10.1161/CIRCULATIONAHA.111.064030

Christensen, J.L., and I.L. Weissman. 2001. Flk-2 is a marker in hematopoietic stem cell differentiation: a simple method to isolate long-term stem cells. *Proc. Natl. Acad. Sci. USA*. 98:14541–14546. http://dx.doi.org/10.1073/pnas.261562798

Colonna, M., J. Samaridis, and L. Angman. 2000. Molecular characterization of two novel C-type lectin-like receptors, one of which is selectively expressed in human dendritic cells. *Eur. J. Immunol*. 30:697–704. http://dx.doi.org/10.1002/1521-4141(200002)30:2<697::AID-IMMU697>3.0.CO;2-M

de Boer, J., A. Williams, G. Skavdis, N. Harker, M. Coles, M. Tolaini, T. Norton, K. Williams, K. Roderick, A.J. Potocnik, and D. Kioussis. 2003. Transgenic mice with hematopoietic and lymphoid specific expression of Cre. *Eur. J. Immunol*. 33:314–325. http://dx.doi.org/10.1002/immu.200310005

Dzierzak, E., and N.A. Speck. 2008. Of lineage and legacy: the development of mammalian hematopoietic stem cells. *Nat. Immunol*. 9:129–136. http://dx.doi.org/10.1038/ni1560

Essers, M.A., S. Offner, W.E. Blanco-Bose, Z. Waibler, U. Kalinke, M.A. Duchosal, and A. Trumpp. 2009. IFNalpha activates dormant haematopoietic stem cells in vivo. *Nature*. 458:904–908. http://dx.doi.org/10.1038/nature07815

Forsberg, E.C., S.S. Prohaska, S. Katzman, G.C. Heffner, J.M. Stuart, and I.L. Weissman. 2005. Differential expression of novel potential regulators in hematopoietic stem cells. *PLoS Genet*. 1:e28. http://dx.doi.org/10.1371/journal.pgen.0010028

Foudi, A., K. Hochedlinger, D. Van Buren, J.W. Schindler, R. Jaenisch, V. Carey, and H. Hock. 2009. Analysis of histone 2B-GFP retention reveals slowly cycling hematopoietic stem cells. *Nat. Biotechnol*. 27:84–90. http://dx.doi.org/10.1038/nbt.1517

Gazit, R., R. Gruda, M. Elboim, T.I. Arnon, G. Katz, H. Achdout, J. Hanna, U. Qimron, G. Landau, E. Greenbaum, et al. 2006. Lethal influenza infection in the absence of the natural killer cell receptor gene Ncr1. *Nat. Immunol*. 7:517–523. http://dx.doi.org/10.1038/ni1322

Gazit, R., B.S. Garrison, T.N. Rao, T. Shay, J.F. Costello, J. Ericson, F. Kim, J.J. Collins, A. Regev, A.J. Wagers, and D.J. Rossi; Immunological Genome Project Consortium. 2013. Transcriptome analysis identifies regulators of hematopoietic stem and progenitor cells. *Stem Cell Rev*. 1:266–280. http://dx.doi.org/10.1016/j.stemcr.2013.07.004

Goodell, M.A., K. Brose, G. Paradis, A.S. Conner, and R.C. Mulligan. 1996. Isolation and functional properties of murine hematopoietic stem cells that are replicating in vivo. *J. Exp. Med*. 183:1797–1806. http://dx.doi.org/10.1084/jem.183.4.1797

Goyama, S., G. Yamamoto, M. Shimabe, T. Sato, M. Ichikawa, S. Ogawa, S. Chiba, and M. Kurokawa. 2008. Evi-1 is a critical regulator for hematopoietic stem cells and transformed leukemic cells. *Cell Stem Cell*. 3:207–220. http://dx.doi.org/10.1016/j.stem.2008.06.002

Hildebrandt, M., A. Adjei, R. Weinshilboum, J.A. Johnson, D.S. Berlin, T.E. Klein, and R.B. Altman. 2009. Very important pharmacogene summary: sulfotransferase 1A1. *Pharmacogenet. Genomics*. 19:404–406. http://dx.doi.org/10.1097/FPC.0b013e32832e042e

Hosen, N., T. Yamane, M. Muijtjens, K. Pham, M.F. Clarke, and I.L. Weissman. 2007. Bmi-1-green fluorescent protein-knock-in mice

reveal the dynamic regulation of bmi-1 expression in normal and leukemic hematopoietic cells. *Stem Cells*. 25:1635–1644. http://dx.doi.org/10.1634/stemcells.2006-0229

Ivanova, N.B., J.T. Dimos, C. Schaniel, J.A. Hackney, K.A. Moore, and I.R. Lemischka. 2002. A stem cell molecular signature. *Science*. 298:601–604. http://dx.doi.org/10.1126/science.1073823

Kataoka, K., T. Sato, A. Yoshimi, S. Goyama, T. Tsuruta, H. Kobayashi, M. Shimabe, S. Arai, M. Nakagawa, Y. Imai, et al. 2011. Evi1 is essential for hematopoietic stem cell self-renewal, and its expression marks hematopoietic cells with long-term multilineage repopulating activity. *J. Exp. Med.* 208:2403–2416. http://dx.doi.org/10.1084/jem.20110447

Kiel, M.J., O.H. Yilmaz, T. Iwashita, O.H. Yilmaz, C. Terhorst, and S.J. Morrison. 2005a. SLAM family receptors distinguish hematopoietic stem and progenitor cells and reveal endothelial niches for stem cells. *Cell*. 121:1109–1121. http://dx.doi.org/10.1016/j.cell.2005.05.026

Kiel, M.J., O.H. Yilmaz, T. Iwashita, O.H. Yilmaz, C. Terhorst, and S.J. Morrison. 2005b. SLAM family receptors distinguish hematopoietic stem and progenitor cells and reveal endothelial niches for stem cells. *Cell*. 121:1109–1121. http://dx.doi.org/10.1016/j.cell.2005.05.026

Kubota, Y., M. Osawa, L.M. Jakt, K. Yoshikawa, and S. Nishikawa. 2009. Necdin restricts proliferation of hematopoietic stem cells during hematopoietic regeneration. *Blood*. 114:4383–4392. http://dx.doi.org/10.1182/blood-2009-07-230292

Kühn, R., F. Schwenk, M. Aguet, and K. Rajewsky. 1995. Inducible gene targeting in mice. *Science*. 269:1427–1429. http://dx.doi.org/10.1126/science.7660125

Kurogane, Y., M. Miyata, Y. Kubo, Y. Nagamatsu, R.K. Kundu, A. Uemura, T. Ishida, T. Quertermous, K.I. Hirata, and Y. Rikitake. 2012. FGD5 mediates proangiogenic action of vascular endothelial growth factor in human vascular endothelial cells. *Arterioscler. Thromb. Vasc. Biol.* 32:988–996. http://dx.doi.org/10.1161/ATVBAHA.111.244004

Laugwitz, K.L., A. Moretti, J. Lam, P. Gruber, Y. Chen, S. Woodard, L.Z. Lin, C.L. Cai, M.M. Lu, M. Reth, et al. 2005. Postnatal isl1+ cardioblasts enter fully differentiated cardiomyocyte lineages. *Nature*. 433:647–653. http://dx.doi.org/10.1038/nature03215

Luckey, C.J., D. Bhattacharya, A.W. Goldrath, I.L. Weissman, C. Benoist, and D. Mathis. 2006. Memory T and memory B cells share a transcriptional program of self-renewal with long-term hematopoietic stem cells. *Proc. Natl. Acad. Sci. USA*. 103:3304–3309. http://dx.doi.org/10.1073/pnas.0511137103

Matsumoto, A., S. Takeishi, T. Kanie, E. Susaki, I. Onoyama, Y. Tateishi, K. Nakayama, and K.I. Nakayama. 2011. p57 is required for quiescence and maintenance of adult hematopoietic stem cells. *Cell Stem Cell*. 9:262–271. http://dx.doi.org/10.1016/j.stem.2011.06.014

Medvinsky, A., and E. Dzierzak. 1996. Definitive hematopoiesis is autonomously initiated by the AGM region. *Cell*. 86:897–906. http://dx.doi.org/10.1016/S0092-8674(00)80165-8

Montgomery, R.K., D.L. Carlone, C.A. Richmond, L. Farilla, M.E. Kranendonk, D.E. Henderson, N.Y. Baffour-Awuah, D.M. Ambruzs, L.K. Fogli, S. Algra, and D.T. Breault. 2011. Mouse telomerase reverse transcriptase (mTert) expression marks slowly cycling intestinal stem cells. *Proc. Natl. Acad. Sci. USA*. 108:179–184. http://dx.doi.org/10.1073/pnas.1013004108

Morita, Y., H. Ema, S. Yamazaki, and H. Nakauchi. 2006. Non-side-population hematopoietic stem cells in mouse bone marrow. *Blood*. 108:2850–2856. http://dx.doi.org/10.1182/blood-2006-03-010207

Morita, Y., H. Ema, and H. Nakauchi. 2010. Heterogeneity and hierarchy within the most primitive hematopoietic stem cell compartment. *J. Exp. Med.* 207:1173–1182. http://dx.doi.org/10.1084/jem.20091318

Muller-Sieburg, C.E., C.A. Whitlock, and I.L. Weissman. 1986. Isolation of two early B lymphocyte progenitors from mouse marrow: a committed pre-pre-B cell and a clonogenic Thy-1-lo hematopoietic stem cell. *Cell*. 44:653–662. http://dx.doi.org/10.1016/0092-8674(86)90274-6

Nombela-Arrieta, C., G. Pivarnik, B. Winkel, K.J. Canty, B. Harley, J.E. Mahoney, S.Y. Park, J. Lu, A. Protopopov, and L.E. Silberstein. 2013. Quantitative imaging of haematopoietic stem and progenitor cell localization and hypoxic status in the bone marrow microenvironment. *Nat. Cell Biol.* 15:533–543. http://dx.doi.org/10.1038/ncb2730

Ooi, A.G., H. Karsunky, R. Majeti, S. Butz, D. Vestweber, T. Ishida, T. Quertermous, I.L. Weissman, and E.C. Forsberg. 2009. The adhesion molecule esam1 is a novel hematopoietic stem cell marker. *Stem Cells*. 27:653–661. http://dx.doi.org/10.1634/stemcells.2008-0824

Osawa, M., K. Hanada, H. Hamada, and H. Nakauchi. 1996. Long-term lymphohematopoietic reconstitution by a single CD34-low/negative hematopoietic stem cell. *Science*. 273:242–245. http://dx.doi.org/10.1126/science.273.5272.242

Park, I.K., Y. He, F. Lin, O.D. Laerum, Q. Tian, R. Bumgarner, C.A. Klug, K. Li, C. Kuhr, M.J. Doyle, et al. 2002. Differential gene expression profiling of adult murine hematopoietic stem cells. *Blood*. 99:488–498. http://dx.doi.org/10.1182/blood.V99.2.488

Park, I.K., D. Qian, M. Kiel, M.W. Becker, M. Pihalja, I.L. Weissman, S.J. Morrison, and M.F. Clarke. 2003. Bmi-1 is required for maintenance of adult self-renewing haematopoietic stem cells. *Nature*. 423:302–305. http://dx.doi.org/10.1038/nature01587

Pászty, C., N. Mohandas, M.E. Stevens, J.F. Loring, S.A. Liebhaber, C.M. Brion, and E.M. Rubin. 1995. Lethal alpha-thalassaemia created by gene targeting in mice and its genetic rescue. *Nat. Genet.* 11:33–39. http://dx.doi.org/10.1038/ng0995-33

Pineault, N., C.D. Helgason, H.J. Lawrence, and R.K. Humphries. 2002. Differential expression of Hox, Meis1, and Pbx1 genes in primitive cells throughout murine hematopoietic ontogeny. *Exp. Hematol.* 30:49–57. http://dx.doi.org/10.1016/S0301-472X(01)00757-3

Raftogianis, R.B., T.C. Wood, D.M. Otterness, J.A. Van Loon, and R.M. Weinshilboum. 1997. Phenol sulfotransferase pharmacogenetics in humans: association of common SULT1A1 alleles with TS PST phenotype. *Biochem. Biophys. Res. Commun.* 239:298–304. http://dx.doi.org/10.1006/bbrc.1997.7466

Rossi, D.J., D. Bryder, J.M. Zahn, H. Ahlenius, R. Sonu, A.J. Wagers, and I.L. Weissman. 2005. Cell intrinsic alterations underlie hematopoietic stem cell aging. *Proc. Natl. Acad. Sci. USA*. 102:9194–9199. http://dx.doi.org/10.1073/pnas.0503280102

Seita, J., D. Sahoo, D.J. Rossi, D. Bhattacharya, T. Serwold, M.A. Inlay, L.I. Ehrlich, J.W. Fathman, D.L. Dill, and I.L. Weissman. 2012. Gene Expression Commons: an open platform for absolute gene expression profiling. *PLoS ONE*. 7:e40321. http://dx.doi.org/10.1371/journal.pone.0040321

Shojaei, F., J. Trowbridge, L. Gallacher, L. Yuefei, D. Goodale, F. Karanu, K. Levac, and M. Bhatia. 2005. Hierarchical and ontogenic positions serve to define the molecular basis of human hematopoietic stem cell behavior. *Dev. Cell*. 8:651–663. http://dx.doi.org/10.1016/j.devcel.2005.03.004

Siminovitch, L., E.A. McCulloch, and J.E. Till. 1963. The Distribution of Colony-Forming Cells among Spleen Colonies. *J. Cell. Physiol.* 62:327–336. http://dx.doi.org/10.1002/jcp.1030620313

Sobanov, Y., A. Bernreiter, S. Derdak, D. Mechtcheriakova, B. Schweighofer, M. Düchler, F. Kalthoff, and E. Hofer. 2001. A novel cluster of lectin-like receptor genes expressed in monocytic, dendritic and endothelial cells maps close to the NK receptor genes in the human NK gene complex. *Eur. J. Immunol.* 31:3493–3503. http://dx.doi.org/10.1002/1521-4141(200112)31:12<3493::AID-IMMU3493>3.0.CO;2-9

Spangrude, G.J., S. Heimfeld, and I.L. Weissman. 1988. Purification and characterization of mouse hematopoietic stem cells. *Science*. 241:58–62. http://dx.doi.org/10.1126/science.2898810

Suzuki, N., O. Ohneda, N. Minegishi, M. Nishikawa, T. Ohta, S. Takahashi, J.D. Engel, and M. Yamamoto. 2006. Combinatorial Gata2 and Sca1 expression defines hematopoietic stem cells in the bone marrow niche. *Proc. Natl. Acad. Sci. USA*. 103:2202–2207. http://dx.doi.org/10.1073/pnas.0508928103

Tadjali, M., S. Zhou, J. Rehg, and B.P. Sorrentino. 2006. Prospective isolation of murine hematopoietic stem cells by expression of an Abcg2/GFP allele. *Stem Cells*. 24:1556–1563. http://dx.doi.org/10.1634/stemcells.2005-0562

Taoudi, S., C. Gonneau, K. Moore, J.M. Sheridan, C.C. Blackburn, E. Taylor, and A. Medvinsky. 2008. Extensive hematopoietic stem cell generation in the AGM region via maturation of VE-cadherin+CD45+ pre-definitive HSCs. *Cell Stem Cell*. 3:99–108. http://dx.doi.org/10.1016/j.stem.2008.06.004

Thebault, P., N. Lhermite, G. Tilly, L. Le Texier, T. Quillard, M. Heslan, I. Anegon, J.P. Soulillou, S. Brouard, B. Charreau, et al. 2009. The C-type lectin-like receptor CLEC-1, expressed by myeloid cells and endothelial cells, is up-regulated by immunoregulatory mediators and moderates T cell activation. *J. Immunol.* 183:3099–3108. http://dx.doi.org/10.4049/jimmunol.0803767

Till, J.E., and E.A. McCulloch. 1961. A direct measurement of the radiation sensitivity of normal mouse bone marrow cells. *Radiat. Res.* 14:213–222. http://dx.doi.org/10.2307/3570892

Tumbar, T., G. Guasch, V. Greco, C. Blanpain, W.E. Lowry, M. Rendl, and E. Fuchs. 2004. Defining the epithelial stem cell niche in skin. *Science.* 303:359–363. http://dx.doi.org/10.1126/science.1092436

Wakabayashi, Y., H. Watanabe, J. Inoue, N. Takeda, J. Sakata, Y. Mishima, J. Hitomi, T. Yamamoto, M. Utsuyama, O. Niwa, et al. 2003. Bcl11b is required for differentiation and survival of alphabeta T lymphocytes. *Nat. Immunol.* 4:533–539. http://dx.doi.org/10.1038/ni927

Weissman, I.L. 2000. Stem cells: units of development, units of regeneration, and units in evolution. *Cell.* 100:157–168. http://dx.doi.org/10.1016/S0092-8674(00)81692-X

Weksberg, D.C., S.M. Chambers, N.C. Boles, and M.A. Goodell. 2008. CD150- side population cells represent a functionally distinct population of long-term hematopoietic stem cells. *Blood.* 111:2444–2451. http://dx.doi.org/10.1182/blood-2007-09-115006

Wilborn, T.W., K.A. Comer, T.P. Dooley, I.M. Reardon, R.L. Heinrikson, and C.N. Falany. 1993. Sequence analysis and expression of the cDNA for the phenol-sulfating form of human liver phenol sulfotransferase. *Mol. Pharmacol.* 43:70–77.

Wilson, A., E. Laurenti, G. Oser, R.C. van der Wath, W. Blanco-Bose, M. Jaworski, S. Offner, C.F. Dunant, L. Eshkind, E. Bockamp, et al. 2008. Hematopoietic stem cells reversibly switch from dormancy to self-renewal during homeostasis and repair. *Cell.* 135:1118–1129. http://dx.doi.org/10.1016/j.cell.2008.10.048

Wolf, N.S., A. Koné, G.V. Priestley, and S.H. Bartelmez. 1993. In vivo and in vitro characterization of long-term repopulating primitive hematopoietic cells isolated by sequential Hoechst 33342-rhodamine 123 FACS selection. *Exp. Hematol.* 21:614–622.

Yokota, T., K. Oritani, S. Butz, K. Kokame, P.W. Kincade, T. Miyata, D. Vestweber, and Y. Kanakura. 2009. The endothelial antigen ESAM marks primitive hematopoietic progenitors throughout life in mice. *Blood.* 113:2914–2923. http://dx.doi.org/10.1182/blood-2008-07-167106

Zhou, B., Q. Ma, S. Rajagopal, S.M. Wu, I. Domian, J. Rivera-Feliciano, D. Jiang, A. von Gise, S. Ikeda, K.R. Chien, and W.T. Pu. 2008. Epicardial progenitors contribute to the cardiomyocyte lineage in the developing heart. *Nature.* 454:109–113. http://dx.doi.org/10.1038/nature07060

Zou, P., H. Yoshihara, K. Hosokawa, I. Tai, K. Shinmyozu, F. Tsukahara, Y. Maru, K. Nakayama, K.I. Nakayama, and T. Suda. 2011. p57(Kip2) and p27(Kip1) cooperate to maintain hematopoietic stem cell quiescence through interactions with Hsc70. *Cell Stem Cell.* 9:247–261. http://dx.doi.org/10.1016/j.stem.2011.07.003